Applied Energy 382 (2025) 125031

Contents lists available at ScienceDirect

Applied Energy

journal homepage: www.elsevier.com/locate/apenergy

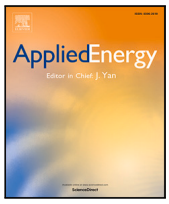

Integration of offshore energy into national energy system: A case study on Belgium

Jocelyn Mbenoun [a], Amina Benzerga [a], Bardhyl Miftari [a], Ghislain Detienne [b], Thierry Deschuyteneer [b], Juan Vazquez [b], Guillaume Derval [a,*], Damien Ernst [a,c]

[a] Montefiore Institute, Liège, Belgium
[b] Fluxys, Belgium
[c] LTCI, Télécom Paris, Institut Polytechnique de Paris, France

ARTICLE INFO

Keywords:
Graph-based optimisation modelling language
Energetic system modelling
Offshore hub
Hydrogen
Multi-energy system

ABSTRACT

Offshore wind farms are typically connected to the mainland via HVAC or HVDC lines. Another possibility to transmit energy is using molecules instead of electricity which may lead to reduced cost and better storage opportunities. This paper proposes a multi-carrier (natural gas, electricity and hydrogen) model of the Belgium energy system in 2050, under carbon neutrality constraint, to assess whether an energy mix should contain offshore hydrogen production. While HV lines remain the main way of transmitting energy from the offshore farm to mainland, the results show that depending on the renewable capacities, the distance between the wind farm and the coast, and the price of hydrogen import, producing H_2 offshore could be beneficial.

1. Introduction

The European Commission has targeted carbon neutrality in EU27 by 2050. In this regard, several scenarios have been proposed to reach the set targets by different actors, such as academics, industries, TSO of gas and electricity [1–4]. All these scenarios stress the importance of increasing renewable energy production. The same applies for the Belgium energy transition which possesses a moderate but not yet reached potential in offshore wind energy and still have room to increase its onshore wind and solar PV energy production [5].

Another part of the solution to achieve carbon neutrality is the decarbonisation of certain sectors, especially the heating, transport, and industry sectors. One of the fastest ways it could be achieved is through electrification. Electric vehicles and heat pumps are already mature technologies and are more efficient than their fossil fuels and gas-fuelled counterparts [6]. Moreover, both can be used as short-term storage and demand-shifting potential. In the industry sector, electricity can also be used as a source of energy for low-temperature (e.g. heat pump), medium-temperature (e.g. electric infrared heating) or high-temperature (e.g. induction heating, electric arc furnace) heating processes [7].

In this aspect, the Belgium transmission system operator (TSO) Elia has laid plans to develop the Belgian power grid in order to make it ready to cope with the increase in electricity production and consumption [8]. For the development of the high-voltage grid (380 kV), three pillars were identified:

- the development of the offshore network to bundle the connections of additional offshore wind farms and to ensure economically efficient transmission to the land,
- the reinforcement and the extension of interconnection capacity with adjacent countries,
- the reinforcement and extension of the power grid within Belgium.

However, it comes with substantial costs in electrical infrastructure [9].

A solution to mitigate these costs could be to support the decarbonisation by electrification with the use of green molecules (green or blue hydrogen and synthetic methane). Hydrogen is already used as feedstock for iron, steel, ammonia, fuel production and the petrochemical industry, but it is mainly produced through steam methane reforming (SMR) which releases carbon dioxide. Blue hydrogen (connecting a carbon capture unit to the SMR device) or green hydrogen (produced from electrolyser using green electricity) could be used as feedstock instead. Hydrogen can also partially substitute the current use of natural gas for medium and high-temperature processes, as well as its use in power plants and can also be used as fuel for transport [10].

* Corresponding author.
E-mail addresses: jmbenoun@uliege.be (J. Mbenoun), abenzerga@uliege.be (A. Benzerga), bmiftari@uliege.be (B. Miftari), ghislain.detienne@fluxys.com (G. Detienne), thierry.deschuyteneer@fluxys.com (T. Deschuyteneer), juan.vazquez@fluxys.com (J. Vazquez), gderval@uliege.be (G. Derval), dernst@uliege.be (D. Ernst).

https://doi.org/10.1016/j.apenergy.2024.125031
Received 14 March 2024; Received in revised form 20 October 2024; Accepted 25 November 2024
Available online 8 January 2025

Nomenclature

C, c	Set of clusters and cluster index
$\mathcal{E}, e$	Set of hyperedges and hyperedge index
$\mathcal{G}$	Hypergraph with node set $\mathcal{N}$ and edge set $\mathcal{E}$
$\mathcal{I}^n, i$	Set of external variables at node n, and variable index
$\mathcal{N}, n$	Set of nodes and node index
$\mathcal{T}, t$	Set of time periods and time index
e_T, e_H	Tail and head of hyperedge $e \in \mathcal{E}$
$\chi_i^n \in \mathbb{R}_+$	Cost of the commodity i consumed by the node n
$\Delta_{i,+}^n \in [0,1]$	Maximum ramp-up rate for flow i and conversion node n (frac. of capacity per unit time)
$\Delta_{i,-}^n \in [0,1]$	Maximum ramp-down rate for flow i and conversion node n (frac. of capacity per unit time)
$\eta_+^n \in [0,1]$	Charge efficiency of storage node n
$\eta_-^n \in [0,1]$	Discharge efficiency of storage node n
$\eta_S^n \in [0,1]$	Self-discharge rate of storage node n
$\iota_i^n \in \mathbb{R}_+$	Cost related to the CO_2 captured from or released to the atmosphere by the node n
$\mu^n \in [0,1]$	Minimum operating level of conversion node n (fraction of capacity)
$\overline{\kappa}^n \in \mathbb{R}_+$	Maximum capacity of technology n
$\phi_i^n \in \mathbb{R}_+$	Conversion factor between reference flow r and flow i for conversion node n
$\phi_{CO_2}^n \in \mathbb{R}_+$	Conversion factor between carbon dioxide produced and flow i for conversion node n
$\pi_t^n \in [0,1]$	(operational) availability of conversion node n at time t
$\psi_r^n \in [0,1]$	Percentage of the commodity r that need to be self-consumed in the node n for its operation
$\rho^n \in [0,1]$	Charge-to-discharge ratio of storage node n
$\underline{\kappa}^n \in \mathbb{R}_+$	Existing capacity of technology n
$E^n \in \mathbb{R}_+$	Stock capacity of storage node n
$e_t^n \in \mathbb{R}_+$	Inventory level of storage node n at time t
$K^n \in \mathbb{R}_+$	Flow capacity of node n
$q_{i,t}^n \in \mathbb{R}_+$	Flow of commodity i at node n and time t

Synthetic methane can also be used as a substitute for natural gas. It does not require any adaptation from the existing gas network and can be easily stored. Part of the gas network can also be repurposed in order to deliver hydrogen, decreasing the cost of supply of this latter molecule [10]. However, both hydrogen and synthetic methane require specific and expensive infrastructure to be produced. Furthermore, the use of green molecules increases the total energy demand due to the conversion losses during their production [6]. This is the reason why the energy demand in futuristic scenarios assumes a partial electrification for certain sectors and the other part is decarbonised via the consumption of green molecules [1,6]. Those scenarios differ in the proportion of green electrons vs green molecules consumed.

This paper aims to challenge the first pillar of the development of the high-voltage grid according to Elia, more specifically the interconnection between offshore wind farms and inland Belgium. It aims to explore whether transporting a portion of the energy generated by offshore wind turbines to mainland Belgium in the form of green hydrogen or synthetic methane would be more advantageous, rather than solely relying on electricity. To this end, an integrated energy system model divided in three geographical regions called clusters, the offshore hub, the coastal area and the Belgium inland, is designed. The objective of this division is to correctly assess the quantity of energy transferred from the offshore hub to inland Belgium and, as a result, the type of infrastructure needed to transport this energy. The modelling of inland Belgium draws inspiration from the optimisation model created in [11]. This model comprises a wide range of technologies and considers the three energy carriers used to supply energy from the offshore hub (electricity, hydrogen and natural gas/methane) and one additional commodity, the carbon dioxide. The energy demands consider different sectors and scenarios from the 2022 Ten-Year Network Development Plans (TYNDP) of the European Network of Transmission System Operators for electricity (ENTSO-E) and gas (ENTSOG) are used for their annual values [1]. A strong constraint of the model is to reach carbon neutrality with scenarios for the year 2050.

The remainder of this paper is organised as follows. Section 2 reviews related works about integrated energy systems and offshore and remote hubs and highlights the areas to which the present paper contributes. Section 3 discusses the assumptions and features of the model, presents the modelling language used, describes the model formulation and introduces the case studies that will be analysed in Section 4. Section 5 proposes sensitivity analyses and Section 6 describes the limitations of the model.

2. Related works

This paper is related to three bodies of work: integrated energy systems, optimisation tools and integration of offshore energy.

Integrated energy systems are widely used to model and evaluate potential pathways towards carbon emission neutrality. These integrated systems can be viewed as networks of interconnected units or components [12], comprising different energy carriers and are described as planning and control problems. A common way of tackling these problems is mathematical programming, in particular Mixed-Integer Linear Programming (MILP) [13] or Linear Programming (LP) [14]. In mathematical programming, the problems are formulated using variables, constraints and an objective function to optimise.

Different tools can be used to formulate and solve those problems. A comparison of those different tools has been made in [15]. The key elements in this comparison was the fact that these tools could be divided into two classes: Algebraic modelling languages (AMLs) such as AMPL [16] or Pyomo [17] and object-oriented modelling environments (OOMEs) such as PyPSA [18] or Calliope [19]. GBOML is a hybrid modelling tool, in-between AMLs and OOMEs. In this work, we use GBOML. GBOML enables one to encode structure, define templates of technologies, allows reuse and model assembling, i.e. key features that are particularly useful for modelling wide energy systems and enabling their extension.

A comprehensive evaluation of integrated energy systems is provided in [20], offering a critical overview of models and evaluation methodologies aimed at analysing multi-energy systems. These methodologies encompass notions such as energy hubs and microgrids. Additionally, [21] proposes a methodology for the simultaneous optimisation of energy systems involving multiple energy carriers, including electricity, natural gas, and district heating. Authors in [22] survey notable methodologies employed to capture the repercussions of variability in power systems within integrated system models. These methodologies consider temporal aspects and employ simplifying assumptions to render the computational handling of such models feasible. One of these methodologies is implemented in [23], where an innovative operational model encompassing both electrical and gas systems is introduced.

From these methodologies, global-scale multi-energy models have been developed to evaluate the potential of the current energy system

in the transition to sustainable energy. Otsuki and al. [24] develop a global multi-energy model that considers 100 regions. They compute the energy supply for the year 2050, accounting for variable renewable energy technologies, system integration (including batteries, water electrolysis, and flexible charging for electric vehicles). Their findings indicate that a mix of variable renewables, carbon capture and storage (CCS)-equipped thermal power plants, and nuclear power plants is the most cost-effective energy system. However, achieving a 100% renewable energy system poses economic challenges in their model.

In [25], the authors present a global model segmented into 9 major regions, which are further divided into 145 subregions. These subregions are balanced to represent comparable shares of global power demand, population, and land area. Their modelling results show that a carbon-neutral electricity system can be economically feasible worldwide by 2050, with a reasonable total system levelized cost of electricity (LCOE) ranging from 26 to 72 €/MWh, averaging 52 €/MWh (uncertainty range: 45–58 €/MWh). Notably, for both [24,25], network stability requirements were not considered, and uncertainties related to social, technological, and institutional factors were not fully incorporated.

In a country scale, [26] presents an energy system model for Denmark, encompassing various sectors (transport, agriculture, and heating). The objective is to assess the feasibility of achieving a 100% renewable energy system by 2050. Their results suggest that this goal is attainable, leading to a 10.2% reduction in greenhouse gas emissions compared to 2000 levels. However, spatial dimensions (i.e. the division of the country into smaller regions) and network infrastructure costs were not explicitly factored into the model.

For Belgium as well, research papers have explored various scenarios for its energy system. Ref. [11] proposes an integrated energy system involving four commodities: electricity, hydrogen, methane/synthetic gas, and carbon dioxide across different sectors. The results highlight that power-to-gas has a limited role in decarbonising Belgium's energy system within the considered sectors. Moreover, due to restricted renewable potential, results show that post-combustion and direct air capture technologies are essential to achieve deep decarbonisation targets. However, the study only covers a small set of scenarios and lacks spatial dimensions, excluding network limitations as well.

Ref. [3] analyses Belgium's energy system, considering multiple carbon emission targets. It addresses electricity, heat, and mobility demands, incorporating 96 technologies and 24 resources. The authors report that Belgium can generate 42% of its primary energy domestically, and a combination of offshore wind, geothermal potential, and nuclear power can lead to a cost-competitive, very low-carbon society. Similarly to the previous paper [11], spatial dimensions are not included, and infrastructure costs are proportional to renewable energy installation. Emissions account only for resources, excluding construction, end-of-life energy conversion, and trade-related emissions.

While these models offer valuable insights into potential pathways for Belgium's energy transition, none of them explore the option of producing hydrogen directly offshore and then transporting it to the shore in that form. However, the big challenge that comes with large investments in offshore wind power mainly concerns how to smoothly fit the generated electricity into current energy systems. Indeed, wind electricity generation is intermittent and consequently, it does not align with the patterns of the electricity demand.

To address this issue, [27] investigates the optimal operation of a coupled wind-hydrogen system. The system supplies green hydrogen to industrial sites and injects it into the natural gas grid. The electrolyser's sizing is based on excess wind power from wind farms. Preliminary results indicate that net power curtailment can be reduced by up to 63% by utilising excess energy for hydrogen production. However, hydrogen production is limited to the Norther wind farm (350 MW capacity) and does not occur offshore.

Offshore wind generation requires massive grid reinforcements [28]. In this context, green hydrogen produced from offshore wind emerges as a promising solution to overcome these obstacles. Various studies have been carried out to assess the potential benefits of offshore energy hubs that produce hydrogen or other electrofuels directly onsite. The authors in [29] investigate three coupling technologies for hydrogen production from offshore wind turbine farms: central onshore electrolysis, decentralised offshore electrolysis, and centralised offshore electrolysis. Offshore hydrogen pipelines are shown more beneficial for large-scale farms, particularly those with longer offshore distances. The decentralised offshore typology offers flexibility, allowing continuous hydrogen production even if one electrolyser or turbine fails. In contrast, the centralised offshore typology is less complex and can employ electrolysis on a separate offshore platform. However, the study does not explore the decision-making process for choosing between hydrogen production and electricity.

In [30], the lowest cost for green hydrogen achievable is explored using an integrated model that designs both hydrogen and offshore electric power infrastructure. The model considers various electrolyser placements, technologies, and operational modes. Results indicate that different electrolyser types are equally competitive, but offshore electrolysis yields the lowest hydrogen cost (2.4€/kg). Additionally, installing an offshore electrolyser reduces wind electricity costs by up to 13% during peak loads. However, the model simplifies by considering only major system components and does not account for electrical grid services like flexible resources.

Some papers explore other fuel production. The work reported in [31] propose a model that determines production quantities and efficiencies for electricity, hydrogen, and ammonia offshore. Results suggest that energy hubs can be sustainable pillars in future energy systems by enhancing the cost-competitiveness of wind power. Longer transport distances and increased storage capacities make ammonia utilisation more worthwhile.

All these studies offer a techno-economic analysis that evaluates the costs of molecules or electrons but fails to account for the integration of offshore production into an inland energy system. The literature is still missing models that connect a multi-energy offshore hub with a comprehensive inland energy system. This gap is notable because such an interconnection could lead to unforeseen dynamics, not only between the offshore hub and the inland energy system but also in the production of various energy carriers within the model.

In this paper, the objective is to associate a comprehensive Belgium energy system comprising a wide variety of technologies generating electricity, hydrogen and methane and an offshore energy hub producing electricity and green hydrogen. Based on [22], an hourly granularity is considered to capture the intermittence of renewable energy generation. The investment and the dispatch are co-optimised for an entire year and an open-source modelling framework is described.

3. The model

The section discusses the objective of the case study, provides a detailed description of the energy system and the different hypotheses made for each of the technologies.

3.1. Objective

The primary goal of this work is to evaluate the optimal method for transporting offshore energy to shore, whether it should be in the form of molecules (such as hydrogen) or electrons (such as electricity). Since the model includes inland technologies, the impact of transportation methods on these technologies will also be examined. Those assessments will take into account various factors, including transmission efficiency, infrastructure costs, storage requirements, and energy demand patterns, to determine the most cost-effective approach for meeting energy demand. Moreover, the capacity of renewable-based power generation, carbon capture, and sector coupling technologies will be computed to accomplish cross-sector decarbonisation goals for

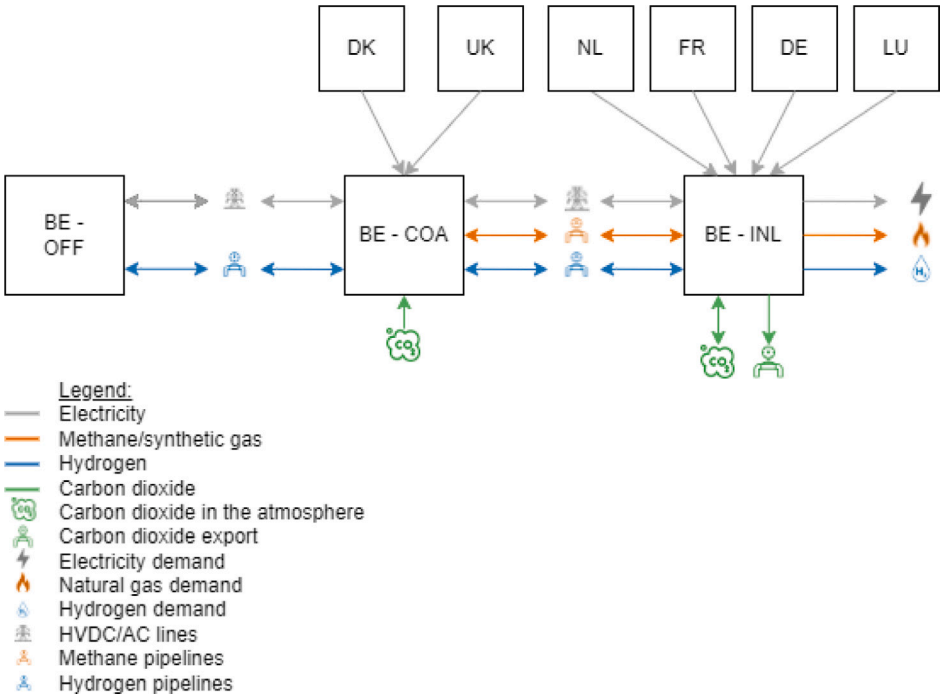

Fig. 1. Simplified representation of the model with the different geographical areas, interconnections and energy flows.

the year 2050 at least cost.

To be able to reach those objectives, a model of the Belgium energy system is developed. The Belgium energy system is split into three distinct geographical regions : the offshore areas (BE-OFF), a transit zone at the coast (BE-COA) and the inland Belgium (BE-INL). The energy demand needs to be satisfied across three energy carriers: electricity, natural gas, and hydrogen. Additionally, the carbon dioxide generated to fulfil these demands is taken into account and can be captured and exported.

3.2. Overall system configuration

The overall architecture of the model is shown in Fig. 1. The three main geographical areas, the offshore area, BE-OFF, the coastal one, BE-COA, and the inland area BE-INL, are displayed, along with the three main commodities (electricity, gas and hydrogen). The neighbouring countries are also displayed.

3.2.1. Geographical areas

The Belgium offshore area. A schema of the offshore area is shown in Fig. 2. It considers two energy vectors, electricity and hydrogen, and one additional commodity, water. There are 7 technologies: wind turbines (WOFF), fuel cells (FC), electrolysis plants (EP), desalination plants (DES), battery storage (BAT), hydrogen storage (H_2St) and water storage (H_2OS). Desalination plants are used to supply water to electrolysers for hydrogen production. Hydrogen storage and fuel cells are considered to compete with electrical batteries for energy storage.

The Belgium coastal area. The Belgium coastal area considers three energy vectors, electricity, hydrogen and natural gas/methane, and one additional commodity, carbon dioxide. By assuming negligible cost and free access to the Belgian water network, water flows are not considered in this cluster. It includes 6 technologies: fuel cells (FC), electrolysis plants (EP), methanation plants (MT), direct air capture (DAC), battery storage. It allows the import of natural gas from Norway (NGNO), the United-Kingdom (NGUK) and France (NGFR), and of synthetic methane by boat (SMI). A schematic representation of the Belgian coastal area is given in Fig. 3.

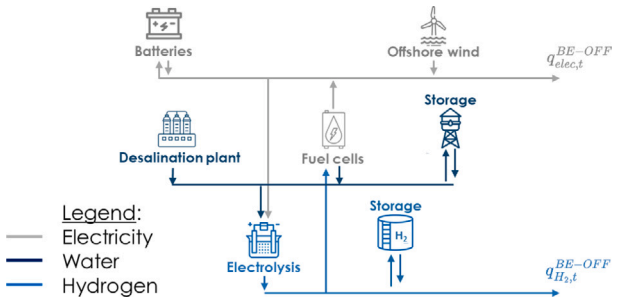

Fig. 2. Schematic representation of the Belgian offshore area.

The Belgium inland area. The Belgium inland area considers three energy vectors, electricity, hydrogen and natural gas/methane, and one additional commodity, the carbon dioxide. Water flows are not modelled for the same reason as in the coastal cluster. It includes 18 technologies: photovoltaic panels (PV), wind turbines (WON), electrolysis plants, fuel cells, direct air capture units, methanation plants, biomethane plants (BMT), combined cycle gas turbines (CCGT), open cycle gas turbines (OCGT), steam methane reformers (SMR), 3 post-combustion carbon capture units (PCCC), battery storage, pumped-hydro power plant (PHP), natural gas storage (CH_4S), hydrogen storage and carbon dioxide storage (CO_2S). Moreover, it considers demand side response such as load shedding (LSd) and load shifting (LSf) for the electricity demand, the linepack of natural gas pipelines (Lp) and natural gas can be imported from Germany (NGDE), hydrogen from Netherlands (H_2NL) and carbon dioxide can be exported (CO_2E). A schematic representation of the Belgian inland area is given in Fig. 4.

3.3. GBOML

In this paper, the Graph-Based optimisation Modelling Language (GBOML version 0.1.7), an open-source software [15], is used to model the energy system. This language enables one to describe an optimisation problem as a hierarchical hypergraph composed of nodes

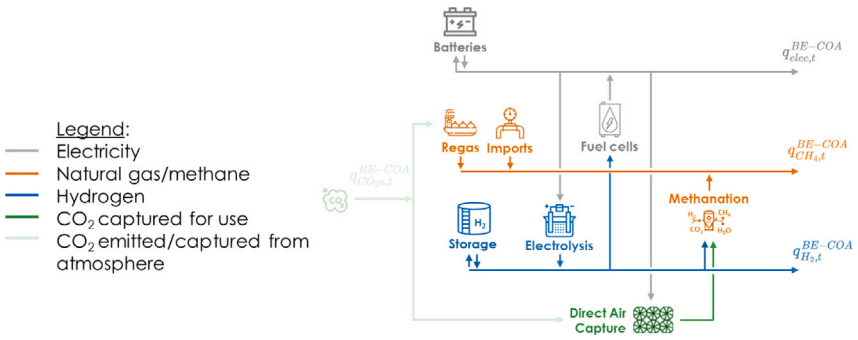

Fig. 3. Schematic representation of the Belgian coastal area.

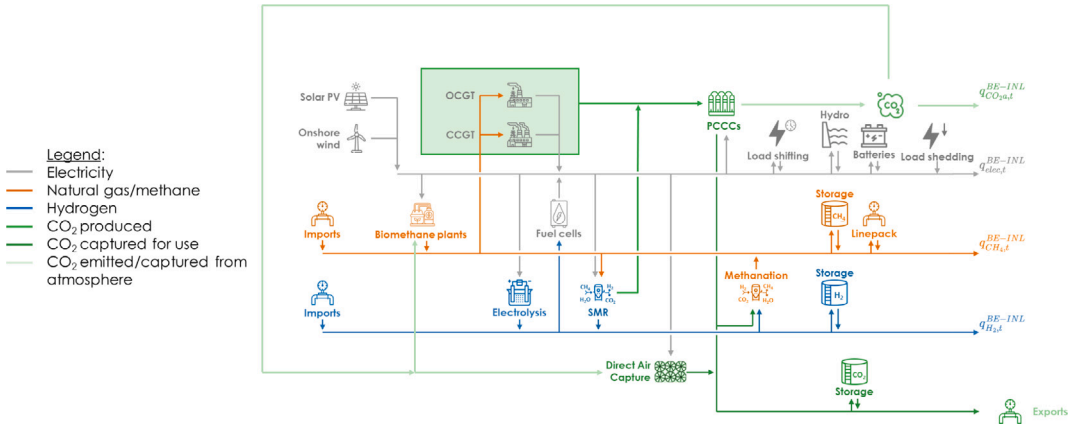

Fig. 4. Schematic representation of the Belgian inland area.

connected by hyperedges. Each node can be seen as an optimisation sub-problem with its own sets of parameters, variables, constraints, local objectives and its own sub-hypergraph. Constraints composed of variables from different nodes can then be defined in a hyperedge to connect different nodes. The objective function of the entire model is the sum of all the objective functions of the different nodes. A detailed mathematical formulation of the GBOML framework is described in Section 3 of [32].

3.4. Modelling assumptions

The mathematical formulation of the energy system in this paper is inspired by [12] where a practical application of GBOML to energy supply chains is described. Nodes typically represent a technology or a process while hyperedges are used to enforce some coupling between nodes. The same principles apply in this paper. Generic nodes model five types of technologies or processes: conversion nodes, flexibility nodes, import/export nodes, transmission nodes and demand nodes. A sixth type, referred to as a cluster, will be a node comprising its own sub-hypergraph (i.e., its own set of nodes and hyperedges), while having its own set of parameters, variables, constraints and objectives. Hyperedges connect nodes and clusters producing/importing or consuming/exporting the same commodity and ensure the balance of flow for each commodity. A global discretised time horizon $T \in \mathbb{N}$ and associated set of time periods $\mathcal{T} = \{0, 1, \ldots, T-1\}$ common to all nodes, are also defined. Similar to [12], parameters are written in Greek letters, sizing variables in capital Latin letters and operation variables in lowercase Latin letters.

A uniform weighted average cost of capital (WACC) of 7% is assumed for all technologies, which corresponds to a situation in which the necessary funds to support the system are obtained through borrowing from capital markets. For nodes producing or importing hydrogen or methane, the parameters in GW or GWh are given for their low heating value (LHV). The objective function of the whole model is the sum of the objective functions of all nodes.

The model is based on four central assumptions:

Central planning and operation. A single entity makes investment and dispatch decisions with the aim of minimising total system cost.

Perfect foresight and knowledge. The entity designing and operating the system has complete knowledge and foresight, thus all technical and economic aspects as well as anticipated weather events and demand patterns are considered as known.

Investment and operational decisions. Investment decisions are made at the start of the time horizon, and assets are immediately available, according to a static investment model. Hourly time steps are used to make operational decisions. Operational and investment decisions are co-optimised in a unique LP problem. Consequently, no market system is considered.

Technology and process models. A set of affine input–output relations that typically express mass and energy balances at the plant or process level are used to model the sizing and operation of technologies. Only storage systems provide a straightforward state space representation, whereas some technologies take into account input or output dynamics.

There are many other assumptions mostly linked to how some technologies are modelled. These are described in the next sections. Of course, all these assumptions induce limitations that will be described in Section 6.

3.5. Conversion nodes

3.5.1. Technologies

Conversion nodes refer to nodes carrying out the conversion of a set of commodities to another via a technology or a process. Conversion

nodes comprise solar panels (PV), onshore wind turbines (WON) and offshore wind turbines (WOFF), nuclear power plants (NK), fuel cells (FC), electrolyser plants (EP), desalination units (DU), methanation plants (MT), direct air capture units (DAC) and biomethane plants (BMT), combined cycle and open cycle gas turbines (CCGT and OCGT respectively), steam methane reformers (SMR) and post combustion carbon capture units (PCCC).

3.5.2. Mathematical formulation

Let $n \in \mathcal{N}$ be a conversion node, commodity flows are modelled as variables, and an index $i \in \mathcal{I}^n$ is assigned to each commodity. For each node n, a reference commodity r is arbitrarily chosen. Let $q^n_{r,t}$ be the flow of the reference commodity $r \in \mathcal{I}^n$ at time t of node n, the flow of all other commodities $q^n_{i,t}$ $\forall i \in \mathcal{I}^n \setminus \{r\}$ of node n is modelled via a set of linear equations which read:

$$q^n_{r,t} = \phi^n_i q^n_{i,t}, \qquad \forall i \in \mathcal{I}^n \setminus \{r\},\ \forall t \in \mathcal{T} \tag{1}$$

where $\phi^n_i \in \mathbb{R}_+$ is the *conversion factor* between commodity r and i (for example in a gas power plant, the commodity r is the electricity produced and i is the gas consumed). In the case of multiple inflows, such as methanation plants, Eq. (1) is applied separately for each distinct inflow. The maximum flow of a reference commodity r is limited by the flow capacity K^n of the technology n such that:

$$q^n_{r,t} \leq \pi^n_t K^n, \qquad \forall t \in \mathcal{T}. \tag{2}$$

$\pi^n_t \in [0,1]$ indicates the maximum production per capacity of technology n at time t; it is typically used to represent exogenous factors such as solar irradiation and wind. The flow capacity K^n is a variable and may be bounded using the constraint:

$$\underline{\kappa}^n \leq K^n \leq \bar{\kappa}^n, \tag{3}$$

where $\underline{\kappa}^n \in \mathbb{R}_+$ represents the existing capacity and $\bar{\kappa}^n \in \mathbb{R}_+$ the maximum capacity of technology n that may be installed. Various operational limitations can also be taken into account. For example, certain conversion technologies may have specific operating ranges and require a minimum flow of commodity $r \in \mathcal{I}^n$ to be maintained in order to function properly. If $\mu^n \in [0,1]$ represents the minimum operating level (as a fraction of the installed capacity), this requirement can be expressed as:

$$\mu^n K^n \leq q^n_{r,t}, \qquad \forall t \in \mathcal{T}. \tag{4}$$

There may also be restrictions on how quickly the flow of commodity $r \in I^n$ can change, which are known as ramping constraints and expressed as:

$$q^n_{r,t} - q^n_{r,t-1} \leq \Delta^n_{r,+} K^n, \qquad q^n_{r,t} - q^n_{r,t-1} \geq -\Delta^n_{r,-} K^n, \qquad \forall t \in \mathcal{T} \setminus \{0\}, \tag{5}$$

with $\Delta^n_{r,+} \in [0,1]$ and $\Delta^n_{r,-} \in [0,1]$ are the maximum rates at which flows can be ramped up and down (as a fraction of the installed capacity per unit time), respectively.

Certain technologies are susceptible to planned outages, which can influence their yearly availability. To address this consideration, a new parameter denoted as $\alpha^n \in [0,1]$ is introduced. This parameter represents the proportion of time within a year, expressed as a percentage, during which outages are assumed to occur for technology n, respectively:

$$\sum_{t \in \mathcal{T}} q^n_{r,t} \leq (1 - \alpha^n) \sum_{t \in \mathcal{T}} K^n. \tag{6}$$

The model can then optimally divide these outages when they have the least impact.

For some nodes, the total amount of their reference commodity is limited by the equation:

$$\sum_{t \in \mathcal{T}} q^n_{r,t} \leq \nu \kappa^n_{tot}, \tag{7}$$

where $\nu \in \mathbb{N}$ is the number of years spanned by the optimisation horizon and κ^n_{tot} is the annual amount of commodity r that can be produced by node n (for example, the amount of biomass may be limited).

The objective function aims to minimise the total costs of each node. Depending on the specific node, different costs must be considered. In this work, we use what we refer to as cost functions to define these costs. The first cost function takes into account the investment, the maintenance and the operation as follows:

$$F^n = \nu(\zeta^n + \theta^n_f)(K^n - \underline{\kappa}^n) + \sum_{t \in \mathcal{T}} \theta^n_v q^n_{r,t} \delta t, \tag{8}$$

where $\nu \in \mathbb{N}$ is the number of years spanned by the optimisation horizon, $\zeta^n \in \mathbb{R}_+$ represents the annualised investment cost, $\theta^n_f \in \mathbb{R}_+$ models fixed operation and maintenance (FOM) costs and $\theta^n_v \in \mathbb{R}_+$ represents variable operation and maintenance (VOM) costs. The annualised investment cost is computed as follows:

$$\zeta^n = CAPEX^n \times \frac{w^n}{1 - (1 + w^n)^{-L^n}}, \tag{9}$$

where $CAPEX^n$ is the capital expenditure, w^n is the weighted average cost of capital (WACC) and L^n is the lifetime of node n.

For certain nodes, a cost function related to an exogenous commodity (that are not considered in the VOM costs) consumed by some technologies (e.g. nuclear power plant) can also be added to the objective to minimise:

$$F^n_i = \chi^n_i \sum_{t \in \mathcal{T}} q^n_{i,t} \delta t, \tag{10}$$

where $\chi^n_i \in \mathbb{R}_+$ is the cost of the commodity i consumed by the node n and $\delta t \in \mathbb{R}_+$ is the duration of each time period

3.5.3. Nodes modelling

Each node is modelled with one variable representing the plant capacity and remaining variables representing different commodity in- and out-flows. Eqs. (1)–(6), with π^n_t being either a time series for intermittent renewable technologies, or equal to 1 for all $t \in \mathcal{T}$ for dispatchable technologies in Eq. (2), and the cost function (8) are used to model those technologies. For offshore electrolysers and fuel cells, an additional cost is factored in to account for the extra installation requirements. For biomethane plants, Eq. (7) limiting its annual production is also used. The annual potential of biomethane produced is based on a study from Valbiom [33]. For NK and BMT, the cost function (10) is also added in the objective function to consider the fuel cost.

Three hypothetical commodities are used to represent carbon dioxide. $CO_{2,g}$ represents carbon dioxide in exhaust gas from combustion processes, $CO_{2,c}$ represents carbon dioxide captured for export or reuse, and $CO_{2,a}$ represents carbon dioxide in the atmosphere. Each unit of $CO_{2,g}$ can either be released into the atmosphere or captured by PCCC units. In these PCCC units, it is assumed that a maximum of 90% of the $CO_{2,g}$ is captured, while the remaining CO_2 is released into the atmosphere.

Technical and economic parameters of all the conversion nodes are presented in Tables 2–4 in Appendix. Almost all parameters are predictions for 2050 from several sources [34–36]. The parameters for both post-combustion carbon capture and desalination units are predictions for 2030 due to a lack of information for 2050 [11,12].

3.6. Flexibility nodes (storage, demand-side response (DSR))

3.6.1. Technologies

A flexibility node plays a crucial role in maintaining equilibrium between production and demand. These nodes encompass various technologies including storage systems, linepack, and demand-side response mechanisms such as load shedding and load shifting. Load shedding refers to the capability of reducing a portion of the electrical demand at a very high price, while load shifting refers to the ability to delay a portion of the demand.

Storage technologies comprise the electrical battery (BAT), pumped-storage hydroelectricity (PHP), methane underground storage (CH_4S), water storage (H_2OS), compressed hydrogen storage (H_2St) and CO_2 storage (CO_2S).

For natural gas pipeline, the linepack, the amount of gas that can be stored in the gas network, is also represented as a node. This amount is based on the actual gas network of Belgium provided by the Belgian gas TSO. It is not considered for hydrogen in this model due to the actual lack of information.

The load shifting, the ability to shift a part of the demand to decrease the peak load, is modelled as an electrical battery with pre-installed capacities that cannot be increased, a limited amount of electricity that can discharged daily and obligation to refill the battery at a certain hour of the day. Load shifting is only applied to electricity, as, to the best of the author's knowledge, it is not used in other sectors in Belgium. For example, the linepack in the gas pipeline already allows for balancing mismatches between the production and consumption of natural gas.

The load shedding, the ability to shed a part of the electric demand for a very high price is modelled as a battery that can only discharge electricity and is refilled at the beginning of the day from an external source. The load shedding is modelled using five different nodes that differ in the number of hours a day their respective share of the load can be shed at their full capacity (1 h, 2 h, 4 h, 8 h and 24 h). The purpose of incorporating load shedding in this model is to avoid the need for additional production capacity that would only be required for short periods each year. Load shedding is triggered by high hourly electricity costs, ranging from 500 €/MWh for the node with 24-h shedding availability to 2500 €/MWh for the node with only one hour of shedding available per day. The amount of electricity that can be shed daily and the cost related to this shedding are based on [8]. Since both natural gas and hydrogen can be fully supplied through imports, load shedding is not considered for these two energy vectors in this model.

3.6.2. Mathematical formulation

Let $n \in \mathcal{N}$ be a *flexibility node*, let $e_t^n \in \mathbb{R}_+$ be the inventory level at time t of node n, the inventory level dynamics is expressed by the equation:

$$e_{t+1}^n = (1-\eta_S^n)e_t^n + \eta_+^n q_{i,t}^n - \frac{1}{\eta_-^n} q_{j,t}^n, \qquad \forall t \in \mathcal{T} \setminus \{T-1\}, \tag{11}$$

where $q_{i,t}^n$ and $q_{j,t}^n \in \mathbb{R}_+$ represent commodity in- and out-flows at time t, respectively. $\eta_S^n \in [0,1]$ is the self-discharge rate per unit of time, $\eta_+^n \in [0,1]$ is the charge efficiency and $\eta_-^n \in [0,1]$ is the discharge efficiency. The maximum inventory level is limited by the stock capacity of the technology $E^n \in \mathbb{R}_+$ modelled as a variable which may be bounded such that:

$$\underline{\epsilon^n} \le E^n \le \overline{\epsilon^n}, \qquad e_t^n \le E^n, \qquad \forall t \in \mathcal{T}, \tag{12}$$

where $\underline{\epsilon^n}$ represents the existing stock capacity and $\bar{\epsilon}^n$ represents the maximum stock capacity that can be installed. The commodity in- and out-flows are limited by the flow capacity of the technology K^n such that:

$$q_{i,t} \le \rho^n K^n, \qquad q_{j,t} \le K^n, \qquad \forall t \in \mathcal{T}, \tag{13}$$

where $\rho^n \in \mathbb{R}_+$ represents the maximum charge-to-discharge ratio. The charge-to-discharge ratio is used when the maximum commodity in- and out-flows are asymmetric. K^n may be bound using either the constraint (3) or can be dependent on the stock capacity such that:

$$K^n = \xi^n E^n, \tag{14}$$

where $\xi \in [0,1]$ is the flow-to-stock ratio capacity of node n.

To avoid edge effects at the last time step of the optimisation in storage operation, the inventory level at the first time step (i.e for $t = 0$), e_0^n is constrained as:

$$e_0^n = (1-\eta_S^n)e_{T-1}^n + \eta_+^n q_{i,T-1}^n + \frac{1}{\eta_-^n} q_{j,T-1}^n. \tag{15}$$

where $q_{i,T-1}^n$ and $q_{j,T-1}^n$ are in the commodity in- and out-flows at the last time step of the optimisation $t = T-1$.

The process of charging a storage system can involve the utilisation of another commodity, represented by $l \in \mathcal{I}^n, l \neq i,j$ (for example, electricity consumed by compressors). This dependency is incorporated into the model through an additional variable $q_{l,t}^n \in \mathbb{R}_+$ and the corresponding equation:

$$q_{l,t}^n = \phi_i^n q_{i,t}^n, \qquad \forall t \in \mathcal{T}. \tag{16}$$

Similar to conversion nodes, new equations are introduced to consider the planned outages of the technology n with:

$$\sum_{t\in\mathcal{T}} q_{i,t}^n \le (1-\alpha^n) \sum_{t\in\mathcal{T}} K^n, \qquad \forall t \in \mathcal{T}, \tag{17}$$

$$\sum_{t\in\mathcal{T}} q_{j,t}^n \le (1-\alpha^n)\rho^n \sum_{t\in\mathcal{T}} K^n, \qquad \forall t \in \mathcal{T}, \tag{18}$$

where $\rho^n \in \mathcal{R}_+$ represents the maximum discharge-to-charge ratio.

Load shifting and linepack can be seen as a storage technology with an obligation to be refilled at a specific hour of the day. Let $\mathcal{T}_D$ be the set of first time periods of every day in the optimisation horizon, $\gamma^n \in [0,23]$ be the hour of the day at which the node n must be refilled then the constraint forcing node n to be refilled is given by:

$$e_{h+\gamma^n}^n = E^n, \qquad \forall h \in \mathcal{T}_D \tag{19}$$

Moreover, for load shifting and linepack, the amount of commodity that can be discharged during a day cannot exceed the amount of the quantity stored at the hour of refill. In other words, only one cycle of charge and discharge is allowed by day. This is modelled by limiting the daily amount of energy discharged using the constraint:

$$\sum_{t=0}^{23} q_{j,h+\gamma^n+t}^n \le E^n, \qquad \forall h \in \mathcal{T}_D. \tag{20}$$

Finally, for load shedding, it can be mathematically expressed as a "discharge flow" of commodity i. The quantity of commodity i that can be shed is also limited using:

$$\sum_{t=0}^{23} q_{i,h+t}^n \le K^n \omega^n, \qquad \forall h \in \mathcal{T}_D, \tag{21}$$

where ω^n is a parameter representing the number of hours by day the load of node n can be shed at its maximum flow capacity. The cost function of the flexibility node n to minimise is defined as in [12]:

$$F^n = \left[\nu(\varsigma^n + \vartheta_f^n)(E^n - \underline{\epsilon^n}) + \sum_{t\in\mathcal{T}} \vartheta_v^n e_t^n \delta t\right] + \left[\nu(\zeta^n + \theta_f^n)(K^n - \underline{\kappa^n}) + \sum_{t\in\mathcal{T}} \theta_v^n q_{i,t}^n \delta t\right] \tag{22}$$

$\varsigma^n \in \mathbb{R}_+$ and $\zeta^n \in \mathbb{R}_+$ represent the stock and flow components of annual investment costs, $\vartheta_f^n \in \mathbb{R}_+$ and $\theta_f^n \in \mathbb{R}_+$ model the stock and flow components of FOM costs, while $\vartheta_v^n \in \mathbb{R}_+$ and $\theta_v^n \in \mathbb{R}_+$ represent the stock and flow components of VOM costs. ς^n and ζ^n are computed using Eq. (9) with CAPEX for the stock and the flow components.

3.6.3. Nodes modelling

Storage. Each of these technologies comprises two sizing variables, the stock capacity and the flow capacity, and three operational variables, the inventory level, and the commodity in- and out-flows. A sixth variable is used to consider the electricity consumption needed for water storage. Eqs. (11)–(18) are used to model each of those technologies. The cost function in Eq. (22) is minimised. For offshore batteries and H_2 storage, an additional cost is factored in to account for the extra installation requirements. Two storage technologies, pumped-storage hydroelectricity at Coo and natural gas storage at Loenhout, have fixed and pre-installed capacities. These capacities cannot be modified by

the model. Note that for this model, a battery with a discharge-to-charge ratio of six was used. As stated in the previous subsection, the discharge-to-charge ratio when the maximum commodity in- and out-flows are asymmetric. In the case of the battery, a discharge-to-charge ratio of 6 means that for a flow capacity of 1 GW, the battery will be able to discharge 1 GWh/h but only charge 1/6 GWh/h. This number is based on the datasheet [37] used to model the batteries.

Linepack (Lp). Only three operational variables, the inventory level, the commodity in- and out-flows, are considered as the flow and the stock capacities cannot be increased (that would mean an increase in the natural gas grid which is not represented in this model) and, therefore, are fixed at their existing capacities. Eqs. (11), (15), (19)–(20) are used to model the linepack and the cost function in Eq. (22) is minimised. The linepack is not modelled for the hydrogen pipeline and CO_2 pipeline as their networks are not computed in this model.

Load shifting (LSf). Similar to linepack, only three operational variables, the inventory level, the commodity in- and out-flows. Only electric demand can be shifted, the amount of electricity that can be shifted daily is based on [8]. Note that, for this study, the shifting cost is assumed to be 100 €/MWh. Eqs. (11), (15), (19)–(20) are used to model the load shifting and the cost function in Eq. (22) is minimised.

Load shedding (LSd). Two variables are used, the flow capacity which is equivalent to the maximum share of the load that can be shed in one hour, and the electricity outflow. In order to keep the problem linear, the total amount of electricity that can be shed during a day by a specific load shedding node is computed by multiplying the total flow capacity by the number of hours this node allows the load to be shed. Only electric demand can be shed and contrary to its shifting, it comes with a cost (the shorter the amount of hours available a day a node of load shedding, the more expensive its use). Eq. (21) is used to model the load shedding and the cost function in Eq. (22) is minimised.

Technical and economic parameters of all flexibility nodes are presented in Tables 5–8 in Appendix. Economical parameters for all flexibility nodes are in 8. Tables 5 and 6 gather the technical parameters for the storage while Table 7 is for linepack, load shifting and load shedding. Those parameters are based either on prediction for the year 2050 from [37] or from [8,11] or [12].

3.7. Import and export nodes

3.7.1. Commodities imported and exported

A node n is an *import node* or *export node* if it imports or exports a commodity i. The import of natural gas is considered only by pipelines in the model. The capacities of the import nodes are limited by the current existing capacities [38]. Depending on the importing country, some nodes of imports are included in the Coastal cluster (Norway (NGNO), United-Kingdom (NGUK) and France (NGFR)) while others are included in the Inland cluster (Germany (NGDE)).

In this paper, the import of synthetic methane is possible by LNG tanker. The capacity of this node is limited by the current capacity and the regasification facilities of the port of Zeebrugge (i.e. the port of Zeebrugge is assumed to be exclusively used for the import of synthetic methane). As synthetic methane is produced remotely from CO_2 captured from the atmosphere based on the model in [12], burning it should not contribute to an increase of CO_2 in the atmosphere. To consider this specificity, the quantity of synthetic methane imported is associated with a quantity of CO_2 captured to compensate for the CO_2 released when the synthetic methane is burned. A cost of 164.8 €/MWh LHV was assumed for the import cost based on [12].

For the import of hydrogen, it is assumed that the pipeline of natural gas connecting the Netherlands with Belgium is repurposed to be able to import hydrogen. According to recent studies [39], a repurposed pipeline of gas can transport a capacity of hydrogen in GW reaching up to 80% of its initial capacity in natural gas. Only green hydrogen is assumed to be imported. An import cost of 75 €/MWh, equivalent to approximately 2.25 €/kg of hydrogen, was considered. This aligns with the projections outlined in [40], estimating hydrogen costs to be between 1.5 to 2.5 €/kg by the year 2040.

Each neighbouring country is modelled as an electricity import node. Denmark, United Kingdom, Netherlands, France, Germany, and Luxembourg are modelled. The import capacity is limited only to renewable and other emission-free capacities of these countries, and only a part of them can be imported. Those emission-free capacities are based on the capacities from [1] for the Distributed Energy scenario. Namely, 1% of the renewable production and 30% of the nuclear production of each neighbouring country can be imported at each time step. These two numbers are chosen arbitrarily.

CO_2 captured by DAC and PCCC is assumed be exported using a CO_2 export node. The capacity of the node is fixed at 3.5 kt/h (about 30 Mt/year) based on the same hypotheses presented in [11].

3.7.2. Mathematical formulation

Let $\underline{\kappa}^n_t \in \mathbb{R}_+$ be the existing flow capacity of node n at each time t (based on the capacity of a pipeline of gas, which will constant, or the amount of renewable energy produced elsewhere, which would be a time series, for example), then the flow of commodity i from the import or export node n is limited with:

$$q^n_{i,t} \leq \underline{\kappa}^n_t, \qquad \forall t \in \mathcal{T}. \tag{23}$$

Unlike for conversion or flexibility nodes, the model is not allowed to invest in additional import or export capacities. The cost function related to the imports/exports to minimise is given by:

$$F^n = \sum_{t\in\mathcal{T}} \sigma^n_t q^n_{i,t} \delta t, \tag{24}$$

where σ^n_t is the cost of import or export of commodity i at time t for node n.

3.7.3. Nodes modelling

Natural gas imports. Only one variable is used, the quantity of natural gas imported. This variable is constrained by Eq. (23) and the cost function is given by Eq. (24). Note that the costs vary over time. Times series computed and provided by the Belgian natural gas TSO for the year 2015 were normalised and then scaled to have an estimated mean value of 50 €/MWh. To this cost, a tariff, reflecting the cost of using the connecting pipeline, has been added and varies from one country to another based on [41].

Synthetic methane imports (SMI). Two variables are used for this node: the amount of synthetic methane imported and the amount of CO_2 captured to produce this methane. Those variables are constrained by Eqs. (23) and (1). The total cost to minimise is given by the cost function (24).

Hydrogen import (H_2NL). One variable is used: the amount of hydrogen imported. This variable is constrained by Eq. (23). The cost function is given by Eq. (24).

Electricity import. In practice, this forms a time series which is actually the parameter $\underline{\kappa}^n_t$ from Eq. (23).

Moreover, the import capacity at any time step is also capped at the capacity of the interconnect between the country and Belgium; this parameter is called $\underline{\kappa}^{n,HV}$. Additionally, the sum of the individual amount of energy imported $q^n_{\text{elec},t}$ is capped to 1% times the total amount of renewable and nuclear energy produced by the country over the time horizon.

The cost of energy is considered constant and is computed as the average cost of the renewable technologies in the neighbouring country and of its nuclear reactors; the cost also comprises half the price of the HV lines, the other half is assumed to be paid by the neighbour. This cost is calculated based on consistent economic assumptions applied to the conversion technologies (detailed costs provided in Table 4 in the

Appendix). It incorporates a CAPEX of 1.5 M€/GW/km, with an FOM cost equivalent to 1.5% of the CAPEX for high-voltage lines. Data used to compute this cost, as well as the cost itself, is presented for each country in Table 10 in Appendix.

Carbon dioxide export (CO_2E). This node uses one variable: the amount of CO_2 exported. This variable is constraint by Eq. (23) and the cost function is given by Eq. (24).

Technical and economic parameters for all import and export nodes are presented in Table 9 in Appendix.

3.8. Transmission nodes

3.8.1. Technologies

Transmission nodes comprise HVAC and HVDC lines, gas pipelines and hydrogen pipelines carrying energy between the three Belgium's clusters.

3.8.2. Mathematical formulation

For each transmission node, two directions are defined, the *forward* and *reverse*. Let $n \in \mathcal{N}$ be a transmission node, let $i \in \mathcal{I}^n$ and $j \in \mathcal{I}^n$ be the indices of the in/outflows of the commodity transported by node n, then the equations governing the transport of the commodity by technology n in the forward direction, indexed f, are:

$$q^n_{i_f,t} \leq K^n, \qquad q^n_{j_f,t} = \phi^n_i q^n_{i_f,t}, \qquad \forall t \in \mathcal{T}. \tag{25}$$

$q^n_{i_f,t}$ and $q^n_{j_f,t} \in \mathbb{R}_+$ are the inflow and outflow of the commodity at time t and $K^n \in \mathbb{R}_+$ is the flow capacity. $\phi^n_i \in [0,1]$ is the loss factor accounting for the losses in the transmission node. Similar to conversion and flexibility nodes, the maximum capacity of a transmission node may be bounded,

$$\underline{\kappa}^n \leq K^n \leq \overline{\kappa}^n, \tag{26}$$

where $\overline{\kappa}^n$ is the maximum capacity of technology n that may be installed. The same equations constraint the flow of commodity in the reverse direction,

$$q^n_{i_r,t} \leq K^n, \qquad q^n_{j_r,t} = \phi^n_i q^n_{i_r,t}, \qquad \forall t \in \mathcal{T}, \tag{27}$$

in which the suffix r instead of the suffix f stands for reverse direction. Similar to the process of charging a storage system, the flow of a commodity can involve the utilisation of another commodity, represented by $l \in \mathcal{I}^n, l \neq i, j$ (for example, electricity consumed by compressors). This dependency is incorporated into the model through an additional variable $q^n_{l,t} \in \mathbb{R}_+$ and the corresponding equation:

$$q^n_{l,t} = \phi^n_l (q^n_{i_f,t} + q^n_{i_r,t}), \qquad \forall t \in \mathcal{T}. \tag{28}$$

The cost function of the transmission node n to minimise is given by:

$$F^n = v(\zeta^n + \theta^n)(K^n - \underline{\kappa}^n) + \sum_{t \in \mathcal{T}} \theta^n_v (q^n_{i_f,t} + q^n_{i_r,t}) \delta t, \tag{29}$$

where $\zeta^n \in \mathbb{R}_+$ is the annualised investment cost, $\theta^n_f \in \mathbb{R}_+$ models fixed operation and maintenance (FOM) costs and $\theta^n_v \in \mathbb{R}_+$ represents variable operation and maintenance (VOM) costs.

3.8.3. Nodes modelling

As stated previously, these nodes allow the flow to be bi-directional using four variables, the inflow and the outflow of the commodity carried by the node in so-called *forward* and *reverse* directions. For this model, flows in the forward direction are flows going from West to East in Fig. 1 while flows going in the reverse direction are going from East to West. Eqs. (25)–(28) are used to model each of those technologies and the cost function (29) is minimised. Technical and economic parameters of all transmission nodes are presented in Tables 11 and 12 in Appendix. The expenses related to HVAC lines are derived from recent projects implemented by the electricity Transmission System Operator (TSO) to enhance capacities between the Offshore area and Belgium Inland. These costs factor in the expenses for cables, their corresponding substations, the offshore platform [42], and associated installations. Similarly, the costs associated with HVDC lines are drawn from [43], encompassing expenses for the offshore platform, VSC (Voltage Source Converter) converters, cables, and their respective installations.

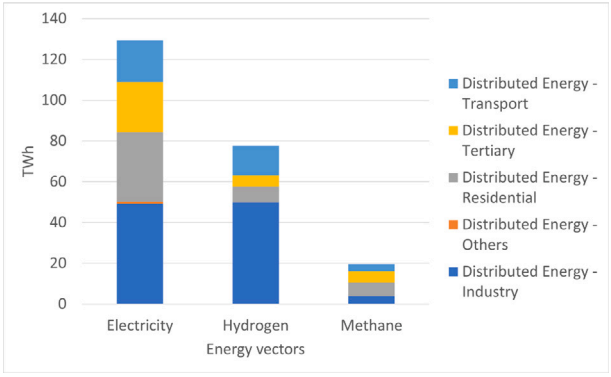

Fig. 5. Belgian final energy demands for each energy vector by sector for the Distributed Energy scenario in 2050 given by the joint TYNDP of ENTSO-E and ENTSOG.

3.9. Demand nodes

3.9.1. Energy carriers

Demands for electricity, natural gas/methane and hydrogen are considered in this model. For each of these commodities, a demand node is designed. Each node considers four sectors: the transport, tertiary, residential and industry sectors. The final energy demands for each energy vector are given for each sector for the year 2050. Their annual values are based on the Joint Scenario Report of the Ten-Year Network Development Plans 2022 (TYNDP) co-written by ENTSOG and ENTSO-E. This report introduces three scenarios built using the supply and demand data collected from both gas and electricity TSOs. Each of these scenarios provides annual predictions for the years 2030, 2040 and 2050. For this paper, the Distributed Energy scenario was chosen as it gives data for the year 2050 and focuses on energy autonomy. The Distributed Energy Scenario was developed using a top-down approach with full-energy perspective while proposing a pathway to reach carbon neutrality by 2050 and a 2030 emission reduction target of at least 55%. Fig. 5 shows the 2050 Belgian annual demands for this scenario.

These annual values are multiplied by normalised time series from Belgian electricity and gas TSO to use realistic profiles. All the time series are taken for the year 2015.

Electrical demand time series. Three time series are used for the electricity demands:

- one time series obtained from estimation made by the Belgian electricity TSO [44] including electrical loads at both transmission and distribution levels, including residential, tertiary (excluding the heating part for these two), industry, aviation and railroad consumption with an annual value of 82.33 TWh;
- one time series obtained from the Belgian gas TSO (Fluxys) for the heating of residential and tertiary sectors with an annual value of 30.58 TWh;
- one synthetic daily profile for electrical-based transportation, assuming a flat daily week-day and week-end travel distances, with a consumption two and a half-times higher for a week-day than for a day in the weekend with an annual value of 16.51 TWh.

Natural gas demand time series. Four time series are used for the natural gas demands:

- one time series from the electronic data platform of the Belgian gas system operator (Fluxys - Belgian's gas TSO) for the industry sector with an annual value of 3.82 TWh;
- another time series from Fluxys for the heating of residential and tertiary sectors with an annual value of 12.22 TWh;
- one time series from confidential data measured by the natural gas TSO at CNG refuelling station for road transport with an annual value of 1.1 TWh;
- a flat profile for the demand related to the shipping sector with an annual value of 2.45 TWh.

Hydrogen demand time series. Four time series are used for the hydrogen demands :

- a flat profile is assumed for the industry sector with an annual value of 49.48 TWh;
- another time series from the Belgian gas TSO for the heating of residential and tertiary sectors with an annual value of 13.24 TWh;
- the same time-series than for the CNG demand is used for the road transport with an annual value of 3.48 TWh;
- a flat time series for the demand is assumed to model the shipping, aviation and rail sectors combined with an annual value of 11.12 TWh.

The costs of energy not served for electricity, hydrogen and natural gas are set to 3000 €/MWh, 500 €/MWh and 500 €/MWh respectively based on values reported for private end users. Eqs. (31)–(32) are used to model the electrical demand node and Eq. (30) is used to model the hydrogen and natural gas demand nodes. For all demand nodes, the cost function (33) is minimised.

3.9.2. Mathematical formulation

Let $n \in \mathcal{N}$ be a demand node, $\lambda^n_{i,s,t}$ be the end user demand for commodity i from time-series s at time t, then $d^n_{i,t}$, the aggregated demand for commodity i at time t, is computed using:

$$d^n_{i,t} = \sum_{s \in S^n_i} \lambda^n_{i,s,t} - l^n_{i,t}, \qquad \forall t \in \mathcal{T}, \tag{30}$$

where S^n_i is the set of all time-series considered for the demand of commodity i and $l^n_{i,t}$ is the energy not served for commodity i at time t. In this model, it is important to note that the electricity demand $g^n_{el,EV,t}$ generated by electric vehicles (EV) is not entirely external. Rather, the model assumes that the timing and intensity of EV charging can be strategically adjusted throughout the day. However, this optimisation is subject to the constraint that a certain daily supply level must be ensured with:

$$\sum_{t=0}^{23} g^n_{el,h+t} = \lambda^n_{el,EV,h}, \qquad \forall h \in \mathcal{T}_D. \tag{31}$$

Subsequently, the aggregated demand for electricity at time t for the node comprising the demand for EV is given by:

$$d^n_{el,t} = \sum_{s \in S^n_{el} \setminus \{EV\}} \lambda^n_{el,s,t} + g^n_{el,t} - l^n_{el,t}, \qquad \forall t \in \mathcal{T}. \tag{32}$$

The cost function of the node to minimise is:

$$F^n = \sum_{t \in \mathcal{T}} \sigma^n_t l^n_{i,t} \delta t, \tag{33}$$

σ^n_t being the cost associated with each quantity of energy not served.

3.10. Clusters

In top of the different nodes, clusters, nodes comprising their own set of nodes and hyperedges are also used to represent each geographical area. From now on, they will be called Offshore cluster, Coastal cluster and Inland cluster. Each of these clusters also has variables and constraints. Those variables represent the net production of the different commodities generated or consumed in the cluster.

For the Offshore cluster, two variables are used. One for the net production of electricity, $q^{BE-OFF}_{elec,t}$ and one for the net production of hydrogen, $q^{BE-OFF}_{h_2,t}$. Fig. 2 presents the technologies used to compute each variable. In the case of fresh water, its production must be equal to its consumption at each time step. An additional constraint is added for this purpose.

For the Coastal cluster, 4 variables are used. One for the net production of electricity, $q^{BE-COA}_{elec,t}$, one for the net production hydrogen, $q^{BE-COA}_{h_2,t}$, one for the net production of methane/natural gas, $q^{BE-COA}_{\mathrm{CH_4},t}$, and one for the carbon dioxide capture from the atmosphere, $q^{BE-COA}_{\mathrm{CO_2}a,t}$. Fig. 3 presents the technologies used to compute each variable. In the case of CO_2 capture for its use, its production must be equal to its consumption at each time step. An additional constraint is added for this purpose.

For the Inland cluster, 5 variables are used. Similar to the coastal cluster, four of them are for the different commodities shown in Fig. 4 : $q^{BE-INL}_{elec,t}$, $q^{BE-INL}_{h_2,t}$, $q^{BE-INL}_{\mathrm{CH_4},t}$, $q^{BE-INL}_{\mathrm{CO_2}a,t}$. An additional constraint is added to preserve the conservation of flow of the CO_2 captured for its use. A fifth variable is considered for the production of electricity, as a constraint limiting it is also considered to simulate the grid limit. It takes into account all the producers minus the consumption of PCCCs connected to power plants at it is assumed that they are directly connected to each other.

3.11. Conservation hyperedges

As stated previously, hyperedges connect nodes and clusters producing/importing or consuming/exporting the same commodity and ensure the balance of flows for each commodity. Some of these flows are also limited by an interconnect capacity; this constraint is added to the hyperedges if needed. Fig. 6 shows the different hyperedges between clusters.

To guarantee carbon neutrality, the model includes a constraint that ensures the net balance of CO_2 — the difference between the total amount of CO_2 emitted into the atmosphere and the total amount of CO_2 captured from the atmosphere — is zero or negative.

In the context of the electrical interconnection linking the Belgium Inland cluster with neighbouring countries and the demand, a constraint has been introduced to restrict the overall flow. This constraints the capacity of the electrical grid to a maximum upper value, which has been fixed in our simulations to 23 GW. This value has been determined by the peak demand in the distributed energy scenario outlined in the TYNDP. Notably, for choosing this value, we did not consider the demand of the transport sector, which, in the scope of this paper, is endogenously managed.

3.12. Objective function

Let $\mathcal{N}$ be the set of all nodes, i.e. conversion, flexibility, import and export, transmission and demand nodes, and $\mathcal{N}_i \subset \mathcal{N}$ a set comprising all conversion nodes consuming an exogenous commodity, the objective function of the entire model is given by

$$\min \sum_{n \in \mathcal{N}} F^n + \sum_{n \in \mathcal{N}_i} F^n_i \tag{34}$$

where F^n is the cost function of node n given in Eqs. (8), (22), (24), (29) or (33) depending on the type of the node, and F^n_i is the cost function related to the consumption of exogenous fuel given in Eq. (10).

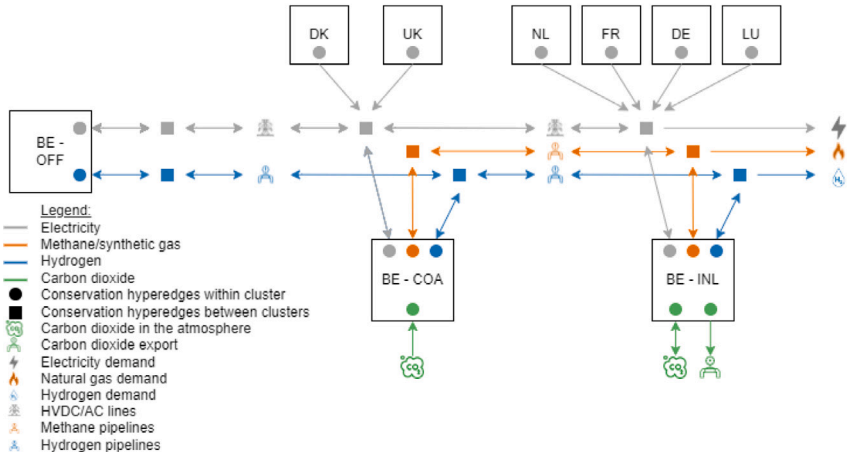

Fig. 6. Schematic representation of the different hyperedges between clusters.

4. Results and discussion

For all simulations, it was assumed that all technologies would be completely replaced by 2050 except for natural gas storage, pumped-hydro power plants, and existing electrical lines and natural gas pipelines within Belgium. The installed capacities of technologies in neighbouring countries were considered constant throughout the optimisation horizon. Moreover, the electrical lines and natural gas pipelines connecting Belgium to its neighbouring countries were assumed to be already established at a fixed capacities, based on future projects proposed by Elia and Fluxys. The pipeline connecting Belgium to the Netherlands was assumed to be repurposed for hydrogen transportation.

4.1. Base scenario

To assess the feasibility of offshore hydrogen production, we simulated two cases. In the first case, only electricity was transported from the offshore site. In the second case, the optimisation model determined the optimal amounts of electricity and hydrogen to be transported from offshore. The installed capacities for each case are illustrated in Figs. 7 and 8.

The results indicate that producing hydrogen offshore is not advantageous under the assumptions of the Base scenario (maximum capacities for selected renewables and the cost of importing H_2). In the second case, only a negligible amount of hydrogen (0.3 TWh/year) is produced offshore compared to the total demand. The rest of the demand is met by the import of hydrogen. The total costs are the same for both cases (20.47 B€/year), with a negligible amount of electricity unmet over the year (9.39 GWh out of 129.42 TWh).

4.2. High renewable scenario

A second scenario was analysed with increased potential for renewable technologies in Belgium. In the Base scenario, the potential for renewable technologies is based on [6]. In the second scenario, referred to as the High Renewable scenario, the potential is based on the study by [5]. Table 1 presents the maximum installable capacities for each scenario.

Similar to the Base scenario, two case studies were examined. In the first, only electricity could be produced and transported from offshore. In the second, the optimisation model determined the optimal amounts of electricity and hydrogen to be transported from offshore to minimise the total cost. Fig. 9 shows the installed capacities and production for each technology in the first case, while Fig. 10 shows them for the second case.

In Fig. 9, due to the increased availability of renewable energy compared to the Base scenario, offshore wind turbines are not installed

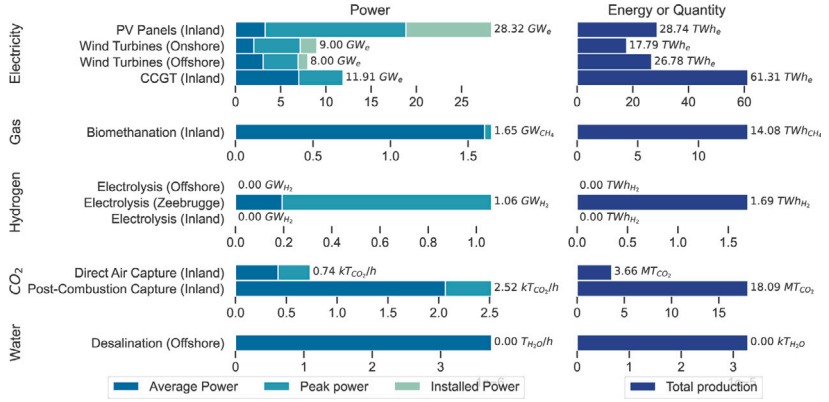

Fig. 7. Installed capacities, peak power, average power and annual production of each conversion nodes when only electricity can be transported from offshore for the Base scenario.

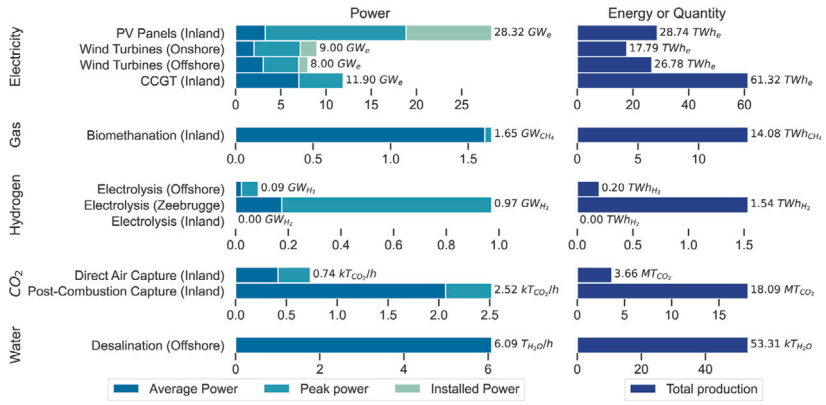

Fig. 8. Installed capacities, peak power, average power and annual production of each conversion nodes when electricity and hydrogen can be transported from offshore for the Base scenario.

Table 1
Maximum capacities of wind turbines in the Offshore cluster, wind turbines in the Inland cluster and the PV in the Inland cluster for each scenario in GW.

	Offshore wind turbines	Onshore wind turbines	PV panels
Scenario 1: Base	8.0	9.0	50.0
Scenario 2: High renewable	9.3	20.5	103.3

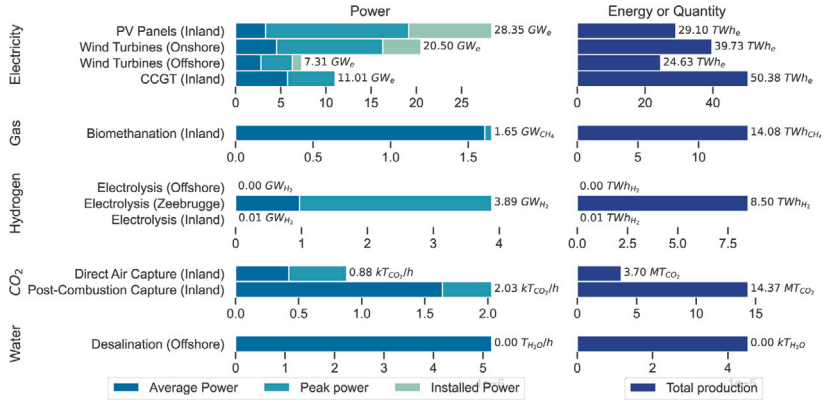

Fig. 9. Installed capacities, peak power, average power and annual production of each conversion nodes when only electricity and hydrogen can be transported from offshore for the High renewable scenario.

at their maximum potential. Onshore wind turbines, being less costly, are preferred, with 20.5 GW installed. Consequently, CCGT capacity is reduced (from nearly 12 GW in the Base scenario to 11 GW in the High Renewable scenario) and they produce much less electricity annually. Hydrogen production at the coast increases significantly, reaching 8.5 TWh annually (compared to only 1.69 TWh in the Base scenario). The total system cost also decreases, from 20.47 B€/year in the Base scenario to 19.88 B€/year. The amount of unmet electricity demand remains negligible, at 39.46 GWh out of 129.42 TWh.

When the model is allowed to transport energy produced offshore in the form of both hydrogen and electricity, offshore wind turbines are installed at their maximum potential, with their capacity factors slightly increasing (from 38.46% to 39.11%). Offshore hydrogen production is introduced, with an installed capacity of 1.56 GW, yielding an annual production of 5.45 TWh. Although coastal electrolysers produce more hydrogen, their capacity factors are much lower than those of offshore electrolysers. Coastal electrolysers produce only 1.5 TWh more annually than offshore electrolysers, despite having more than double the installed capacity of the offshore electrolysers.

It is important to note that no fuel cell is installed. Thus, under the assumptions of this model, converting electricity into hydrogen, storing it, and then converting it back into electricity is not competitive.

Lastly, allowing the transport of hydrogen from offshore results in savings of a bit more than 35 M€/year, with a similar amount of unmet electricity demand.

5. Sensitivity analysis

The production and transportation of hydrogen are central points in the decision to use electrons or hydrogen for offshore energy transportation. Indeed, their costs can be a deterrent and thus lead to the use of electrons. It is therefore important to study the behaviour of factors that influence these costs. In this sensitivity analysis, two factors are studied:

- the impact of the H_2 import price is assessed, which can help identify a threshold beyond which importation is no longer profitable compared to offshore production;
- the distance between offshore and coastal clusters is examined to determine if there exists a distance between these two for which hydrogen pipelines can surpass electrical lines, that are generally more profitable.

This analysis examines both scenarios, focusing first on their effects on offshore installations, followed by the impact of these effects on

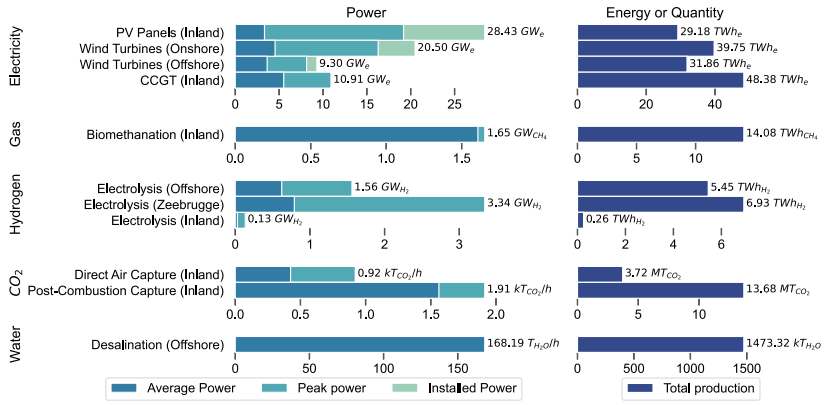

Fig. 10. Installed capacities, peak power, average power and annual production of each conversion nodes when electricity and hydrogen can be transported from offshore for the High renewable scenario.

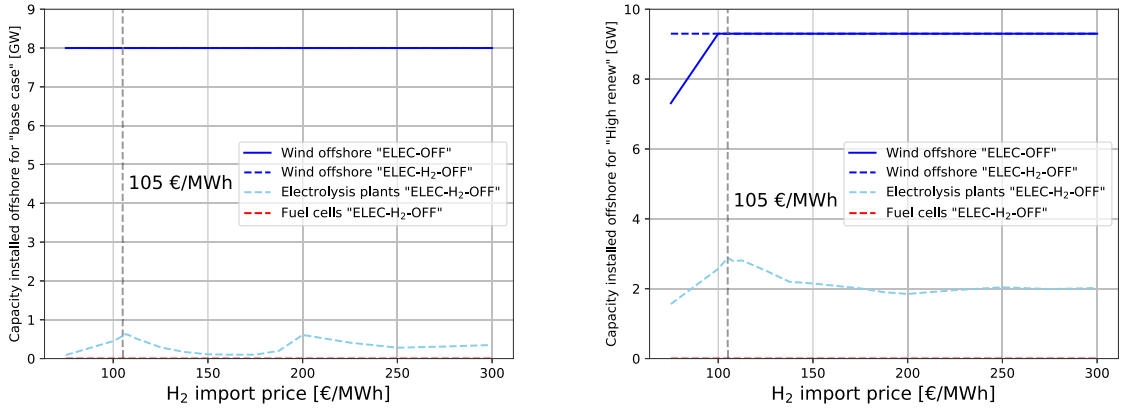

(a) Base scenario. (b) High Renewable scenario.

Fig. 11. Impact of the price of H_2 import on the capacities of offshore technologies. For each scenario, two cases are illustrated: the ELEC-OFF case, where only electricity is generated in the Offshore cluster, represented by solid lines, and the ELEC-H_2-OFF case, where both electricity and hydrogen are generated in the Offshore cluster, shown with dashed lines. For example for the High Renewable scenario, at a H_2 import price of 75 €/MWh, the capacity of wind turbine is 7.31 GW for the case ELEC-OFF and 9.3 GW for the case ELEC-H_2-OFF, and the capacity of electrolysis plant is 1.56 GW for the case ELEC-H_2-OFF.

onshore installations and imports. For each scenario, two cases are considered: one where only electricity is generated in the Offshore cluster (ELEC-OFF), and another where both electricity and hydrogen are produced in the Offshore cluster (ELEC-H_2-OFF).

5.1. Evolution of the price of H_2 imports

For this sensitivity analysis, the price of imported H_2 is increased from 75 €/MWh to 300 €/MWh. Previously, results indicated that at 75 €/MWh, most of the hydrogen consumed was imported. With this increase, it is expected that domestic hydrogen production will rise, eventually becoming the sole source of hydrogen in the model.

5.1.1. Offshore installation

Figs. 11(a) and 11(b) show the evolution of offshore conversion technologies in relation to the price of H_2 imports for both the Base scenario and the High renewable scenario. Each graph provides the capacities of offshore energies producers installed for the case ELEC-OFF and ELEC-H_2-OFF.

In both scenarios, the capacity of offshore electrolysers reaches its maximum value at an H_2 import price of 105 €/MWh. In the High renewable scenario, increasing the H_2 import price encourages the installation of offshore wind turbines to boost green hydrogen production up to 100 €/MWh. From 105 €/MWh to 175 €/MWh, the capacity of electrolysis plants decreases in both scenarios. This is due to the use of steam methane reformers (SMR) at this price point. As SMR also release carbon dioxide, the maximum exportable amount is reached. As the price of hydrogen increases, SMR production ramps up as can be seen in Fig. 12, resulting in more CO_2 emissions, which in turn forces a reduction in combined cycle gas turbine (CCGT) production. To offset this reduction, a portion of the electricity originally used for offshore hydrogen production is redirected for direct electricity use.

Beyond 175 €/MWh, the electrolyser capacities diverge for each scenario. In the Base scenario, electrolyser capacity peaks again at 200 €/MWh, then decreases and stabilises from 250 €/MWh. This new peak occurs because synthetic methane, which is carbon neutral, starts being imported at 175 €/MWh. This allows CCGT to produce more electricity, and some of the electricity from offshore wind turbines can be converted back into hydrogen. In the High Renewable scenario, the capacity of offshore electrolysers stabilises around 2 GW from 175 €/MWh to 300 €/MWh. Thanks to the higher renewable potential, the reduction in CCGT production can be offset by carbon-neutral technologies. As a result, hydrogen production by electrolysers increases in the coastal cluster, driven by additional renewable electricity production, as shown in Fig. 12(b).

5.1.2. Hydrogen production

Figs. 12(a) and 12(b) illustrate the evolution of H_2 production from conversion technologies in the model for both the Base scenario and the High renewable scenario.

Up to 105 €/MWh, only electrolysers produce hydrogen in the model for all cases and scenarios. Beyond 105 €/MWh, steam methane

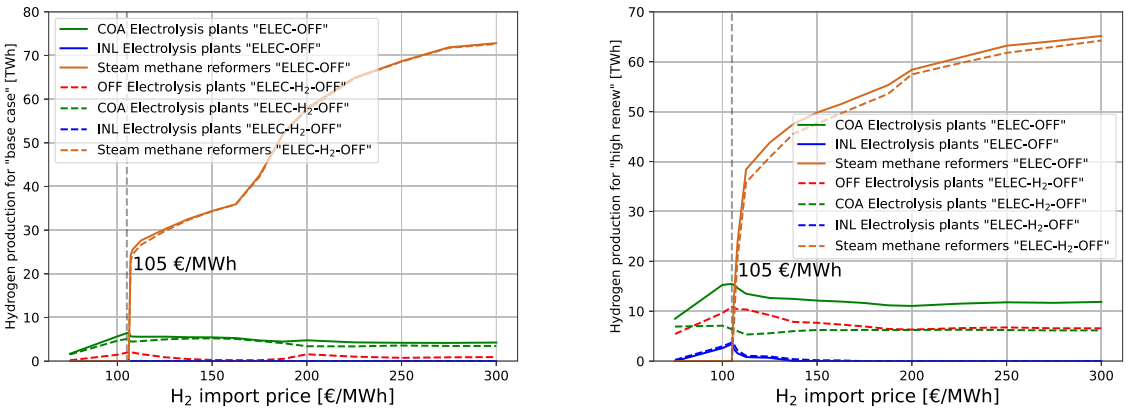

(a) Base scenario. (b) High Renewable scenario.

Fig. 12. Impact of the price of H_2 import on the production of H_2 from hydrogen production technologies. For each scenario, two cases are illustrated: the ELEC-OFF case, where only electricity is generated in the Offshore cluster, represented by solid lines, and the ELEC-H_2-OFF case, where both electricity and hydrogen are generated in the Offshore cluster, shown with dashed lines. Theses graphs can be read the same way as explained in Fig. 11.

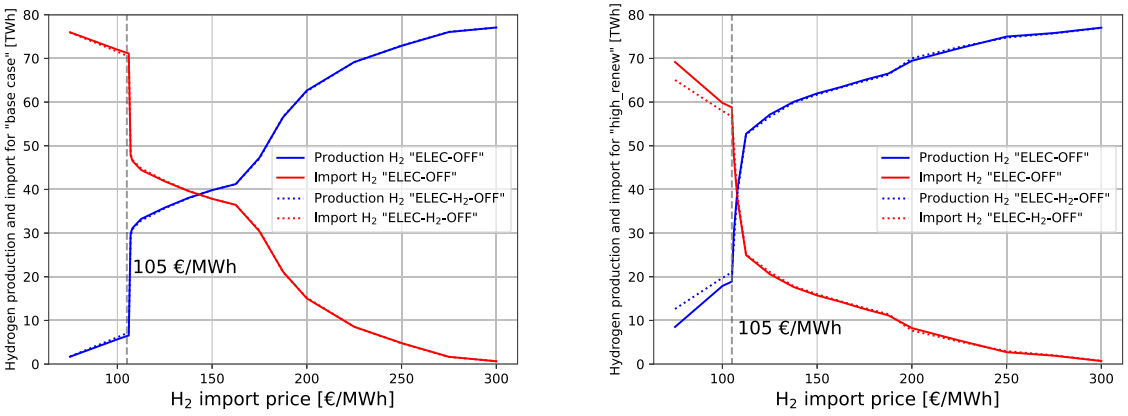

(a) Base scenario. (b) High Renewable scenario.

Fig. 13. Impact of the price of H_2 import on the total production and the import of H_2. For each scenario, two cases are illustrated: the ELEC-OFF case, where only electricity is generated in the Offshore cluster, represented by solid lines, and the ELEC-H_2-OFF case, where both electricity and hydrogen are generated in the Offshore cluster, shown with dashed lines. Theses graphs can be read the same way as explained in Fig. 11.

reformers (SMR) become economically competitive and become the primary hydrogen producers. As the H_2 import price increases, SMR production of H_2 increases correspondingly. Figs. 13(a) and 13(a) show that by 300 €/MWh, hydrogen is almost entirely produced by SMR to meet the demand, with only a negligible amount of hydrogen being imported.

5.1.3. Onshore effects

The graphs in Figs. 14(a) and 14(b) show the evolution of onshore electricity producer installations. The trends are similar for both scenarios, with no significant differences between them. Up to 105€/MWh, only PV and CCGT capacities slightly increase to compensate for the electricity consumption by electrolysers.

From 105 to nearly 200 €/MWh, PV capacities increase and reach their maximum potential in the Base scenario, while CCGT capacity decreases during this interval. The graphs in Figs. 15(a) and 15(b) show that at 105 €/MWh, the total amount of CO_2 imported reaches its maximum value and remains constant for the rest of the sensitivity analysis. This limit explains why the capacities of PV and CCGT decrease. Since SMR is a carbon emitter consuming natural gas, a shift occurs in natural gas consumption between SMR and CCGT. To compensate for this shift, PV installations increase. At 165 €/MWh, the import of green gas becomes cost-competitive in the Base scenario; this occurs slightly later, at 187.5 €/MWh, in the High Renewable scenario.

All capacities for electricity production stabilise between 200 and 300 €/MWh. This is because only the import of synthetic methane increases to supply the SMR that produce hydrogen. By using synthetic methane, the model maintains its carbon neutrality.

5.1.4. Cost differences

Fig. 16 shows the cost difference between the ELEC-OFF and the ELEC-H_2-OFF cases for both the Base scenario and the High renewable scenario.

In both scenarios, the highest difference occurs at 105 €/MWh, just before SMRs start to be installed. For the Base scenario, this difference amounts to 0.038 €/MWh equivalent to 8.5 M€/year, while for the High renewable scenario, it amounts to 0.37 €/MWh, equivalent to 83.96 M€/year.

5.2. Evolution of the distance between offshore and coastal clusters

For this sensitivity analysis, the distance between the offshore and coastal clusters has been increased from 40 to 1000 km. This is expected to impact the cost of the energy interconnectors (H_2 pipelines and HV lines) and favour offshore hydrogen production as the distance increases. For this sensitivity analysis, HVDC lines can also be installed.

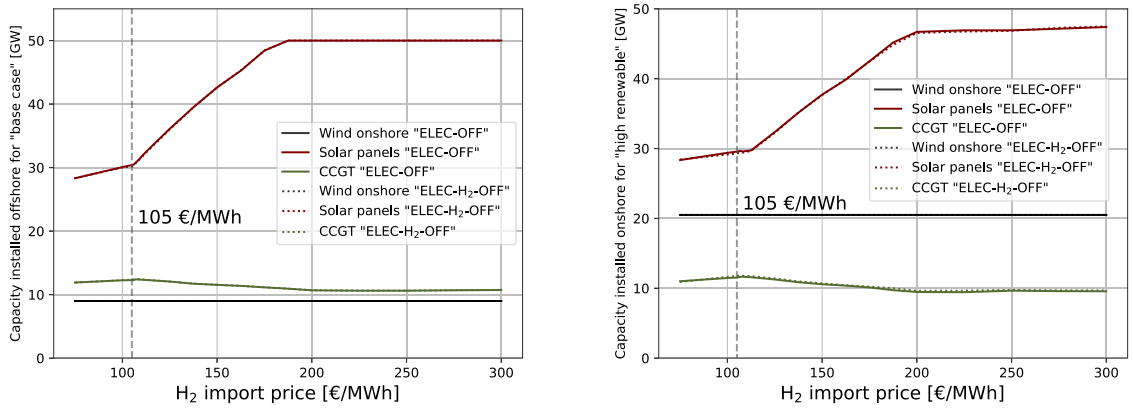

(a) Base scenario. (b) High Renewable scenario.

Fig. 14. Impact of the price of H_2 import on onshore electricity producer installations. For each scenario, two cases are illustrated: the case ELEC-OFF where only electricity can be generated from the Offshore cluster in continuous line and the case ELEC-H_2-OFF, where both electricity and hydrogen can be generated in the Offshore cluster in dashed line. Theses graphs can be read the same way as explained in Fig. 11.

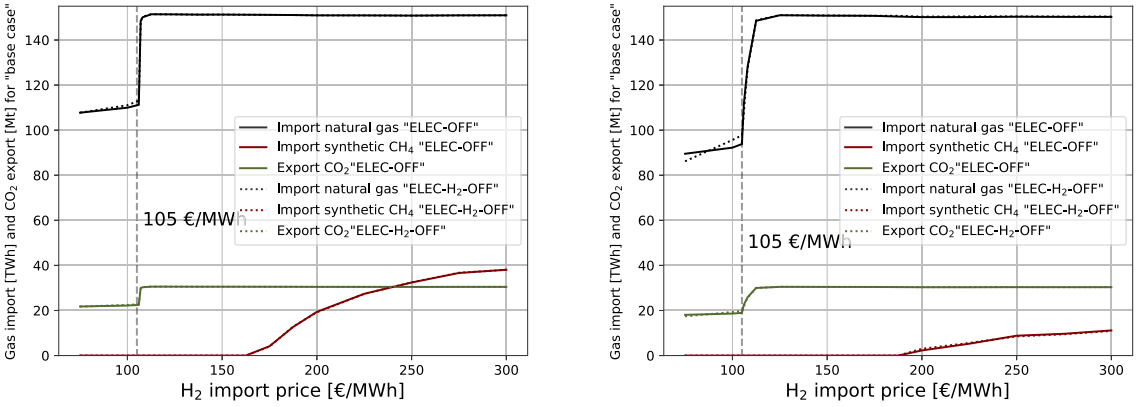

(a) Base scenario. (b) High Renewable scenario.

Fig. 15. Impact of the price of H_2 import on the natural gas and green CH_4 imports and CO_2 export. For each scenario, two cases are illustrated: the ELEC-OFF case, where only electricity is generated in the Offshore cluster, represented by solid lines, and the ELEC-H_2-OFF case, where both electricity and hydrogen are generated in the Offshore cluster, shown with dashed lines. Theses graphs can be read the same way as explained in Fig. 11.

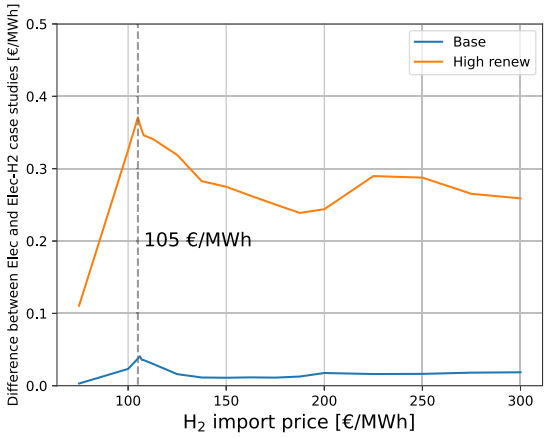

Fig. 16. Evolution of the difference of the cost of energy of the system between the case with offshore electricity production only and combined offshore electricity and hydrogen production for both the Base scenario and the High renewable scenario.

5.2.1. Offshore installations

Figs. 17(a) and 17(b) show the evolution of offshore conversion technologies in relation to the distance between the offshore cluster and the coast for both the Base scenario and the High renewable scenario.

In the Base scenario, producing hydrogen offshore allows the installation of wind turbines to remain viable at maximum capacities up to 750 km. Conversely, if only electricity is produced offshore, wind turbine capacities start to decrease from 200 km and continue to decrease, reaching just over 3 GW at 1000 km. As the distance increases, a larger proportion of the electricity generated by the wind turbines is converted into hydrogen, since installing hydrogen pipelines is less costly. In the High renewable scenario, however, as the distance between the offshore sites and coastal clusters increases, the capacities of both wind turbines and electrolysers decrease.

5.2.2. Hydrogen production

Figs. 18(a) and 18(b) illustrate the evolution of H_2 production from conversion technologies in the model for both the Base scenario and the High renewable scenario.

In the Base scenario, offshore electrolysers quickly become the primary source of hydrogen when permitted. Starting from no production at 40 km, they reach 6 TWh at a distance of 1000 km. Coastal hydrogen production decreases in both cases, dropping to zero at 500 km when hydrogen is produced offshore and at 1000 km when it is not. Additionally, no hydrogen is produced inland, either by electrolyser or steam methane reformer. Overall, as shown in Fig. 19(a), total hydrogen production increases with distance when offshore production is allowed.

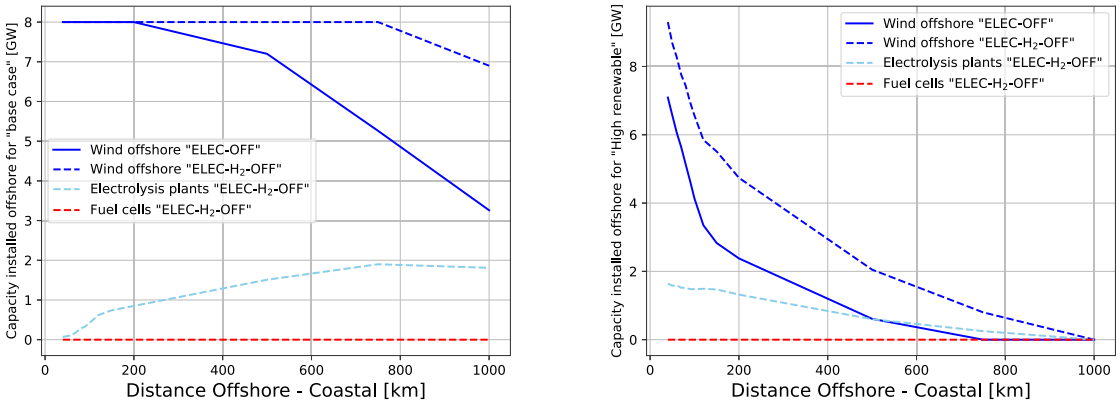

(a) Base scenario. (b) High Renewable scenario.

Fig. 17. Impact of the distance between the offshore and the coastal areas on capacities of offshore technologies. For each scenario, two cases are illustrated: the ELEC-OFF case, where only electricity is generated in the Offshore cluster, represented by solid lines, and the ELEC-H_2-OFF case, where both electricity and hydrogen are generated in the Offshore cluster, shown with dashed lines. Theses graphs can be read the same way as explained in Fig. 11.

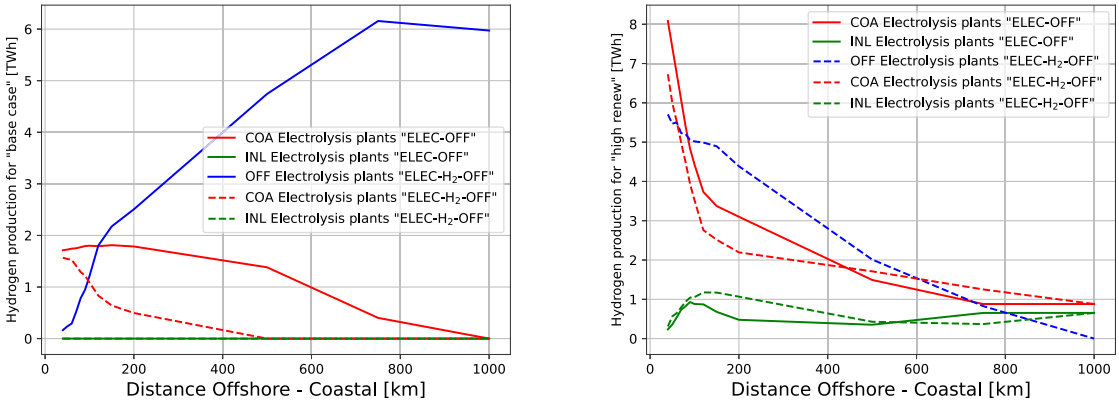

(a) Base scenario. (b) High Renewable scenario.

Fig. 18. Impact of the distance between the offshore and the coastal areas on the production of H_2. For each scenario, two cases are illustrated: the ELEC-OFF case, where only electricity is generated in the Offshore cluster, represented by solid lines, and the ELEC-H_2-OFF case, where both electricity and hydrogen are generated in the Offshore cluster, shown with dashed lines. Theses graphs can be read the same way as explained in Fig. 11.

In the High renewable scenario, as the number of offshore wind turbines decreases, hydrogen production from both offshore and coastal sources also declines as the distance between offshore sites and coastal clusters increases. This reduction is partially offset by a rise in inland electrolyser production. However, as illustrated in Fig. 19(b), total hydrogen production decreases while hydrogen imports increase.

5.2.3. Onshore effects

Figs. 20(a) and 20(b) illustrate the evolution of onshore electricity producer installations in relation to the distance between the offshore cluster and the coast for both the Base scenario and the High renewable scenario.

In the Base scenario, the capacities of Combined Cycle Gas Turbines (CCGT) and Photovoltaics (PVs) increase with distance to compensate for the consumption by electrolysers in both cases. In the High renewable scenario, PV capacities slightly decrease while CCGT capacities increase with distance. The reduction in offshore wind turbine capacities is primarily offset by the increased capacity of CCGTs.

These compensations directly impact the import of molecules, as shown in Figs. 21(a) and 21(b). In both scenarios, the amount of natural gas imported increases with distance to fuel the CCGTs. Consequently, CO_2 exports also rise, as more needs to be captured from the CCGTs.

5.2.4. Cost differences

Fig. 22 shows the cost difference between the ELEC-OFF and the ELEC-H_2-OFF cases for both the Base scenario and the High renewable scenario.

As the distance between offshore and coastal clusters increases, the cost difference becomes more pronounced in the Base scenario, rising to 0.29 €/MWh equivalent to 65.58 M€/year at 750 km. In the High renewable scenario, the cost difference decreases as the number of offshore wind turbines decreases.

6. Limitations

Many hypotheses are scattered throughout the text. For the sake of clarity, we summarise and discuss the main ones here.

In Section 3, we introduce multiple assumptions, which each pose some limitations on the results. The concept of central planning and operation assumes a perfectly competitive market, disregarding the reality of multiple influential actors and factors in the market. Similarly, the perfect foresight and knowledge assumption fail to account for uncertainties in demand, operations, and weather conditions. Moreover, investment and operational decisions rely on a database of cost predictions established in 2021, neglecting recent increases in material costs, and, of course, future unpredictable modifications to these costs in the next years up to 2050. Additionally, assumptions about technologies and processes models overlook startup time, artificially increasing the response time of some technologies. CCGTs, which form a large part of any optimal solution in the model, are modelled such that they need to be running at least at 40% capacity, rather than allowing them to shut

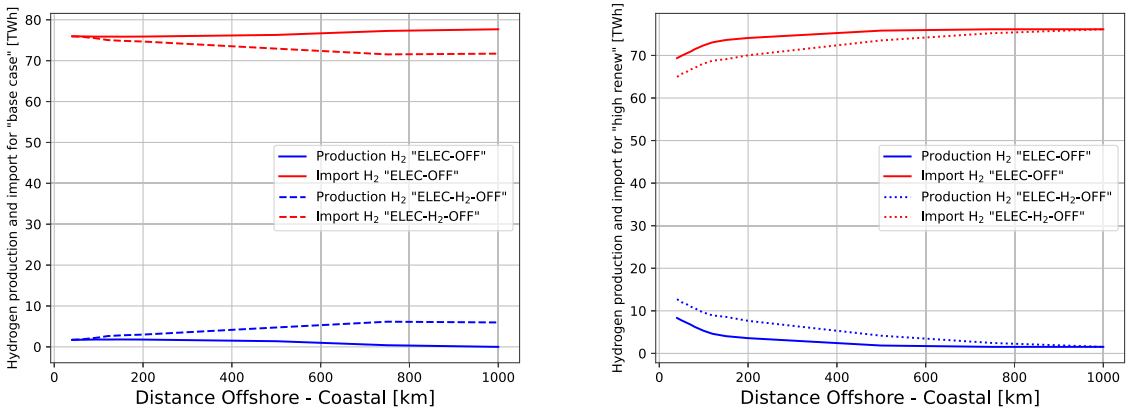

(a) Base scenario. (b) High Renewable scenario.

Fig. 19. Impact of the distance between the offshore and the coastal areas on the total production and the import of H_2. For each scenario, two cases are illustrated: the ELEC-OFF case, where only electricity is generated in the Offshore cluster, represented by solid lines, and the ELEC-H_2-OFF case, where both electricity and hydrogen are generated in the Offshore cluster, shown with dashed lines. Theses graphs can be read the same way as explained in Fig. 11.

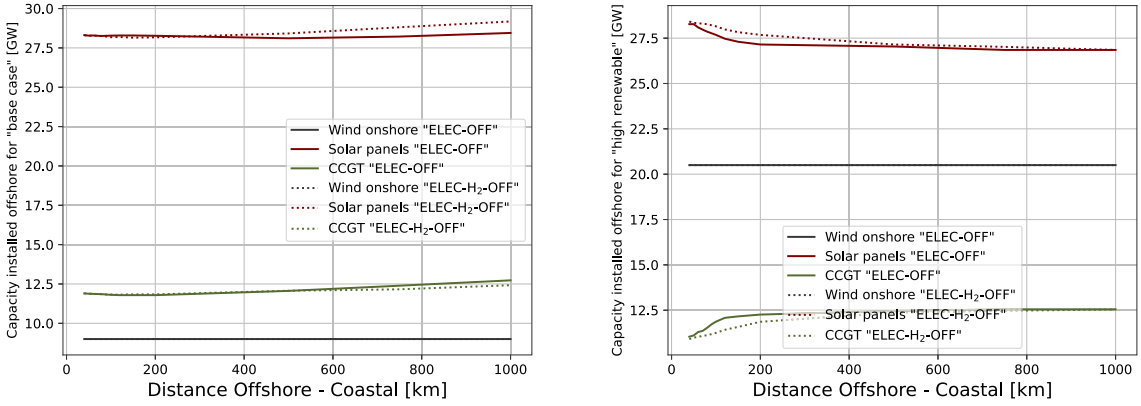

(a) Base scenario. (b) High Renewable scenario.

Fig. 20. Impact of the distance between the offshore and the coastal areas on onshore electricity producer installations. For each scenario, two cases are illustrated: the ELEC-OFF case, where only electricity is generated in the Offshore cluster, represented by solid lines, and the ELEC-H_2-OFF case, where both electricity and hydrogen are generated in the Offshore cluster, shown with dashed lines. Theses graphs can be read the same way as explained in Fig. 11.

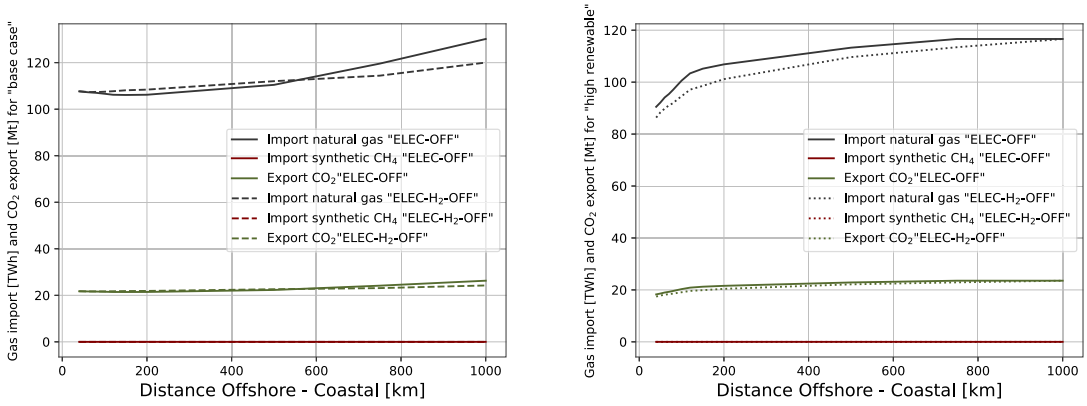

(a) Evolution of natural gas and green CH_4 import and CO_2 export for the Base scenario. (b) Evolution of natural gas and green CH_4 import and CO_2 export for High renewable scenario.

Fig. 21. Impact of the distance between the offshore and the coastal areas on the natural gas and green CH_4 import and CO_2 export. For each scenario, two cases are illustrated: the ELEC-OFF case, where only electricity is generated in the Offshore cluster, represented by solid lines, and the ELEC-H_2-OFF case, where both electricity and hydrogen are generated in the Offshore cluster, shown with dashed lines. Theses graphs can be read the same way as explained in Fig. 11.

down. The above assumptions are employed to maintain the model's size to a manageable one and ensure efficient computations, albeit at the expense of overlooking certain complexities.

A limit was set on the total flow of electricity to avoid unrealistic peaks in the electricity network. A value of 23 GW was decided based on the peak of the electricity demand used in the model. Allowing the

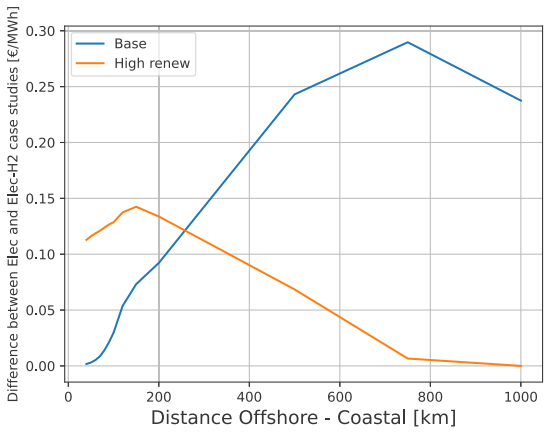

Fig. 22. Evolution of the difference of the cost of energy of the system between the ELEC-OFF case and the ELEC-H_2-OFF case for both the Base scenario and the High renewable scenario.

possibility of increasing this limit with a cost related to an increased capacity could change the results, especially in the number of PVs installed. Another significant limit is on nuclear power generation, which Belgium has currently 4 GW of. Belgium's stance on nuclear power currently excludes it from the country's future electricity production plans. However, plans can change and nuclear energy could still play a significant role in Belgium's hydrogen production—a possibility worth exploring in future research.

Another assumption is that imported electricity comes from decarbonised sources, imposing a cap on the quantity of electricity available for import at each time step. While the model aims to promote local production, other assumptions within it could influence the outcomes.

Gas imports are solely restricted by pipeline capacity, and Belgium, serving as a transit nation, mostly imports natural gas that is subsequently exported to other countries. This limitation in practice affects the volume of natural gas and influences its pricing [45]. A comprehensive investigation would be necessary, although it falls beyond the scope of this paper.

The energy demand relies on TYNDP predictions [1], but it is important to note that demand and supply are related. A rise in costs typically leads to a drop in consumption. Estimating the elasticity of the supply–demand curve is beyond this paper's scope; for simplicity, demands are not influenced by prices and other factors in the model.

Another important assumption was the possibility to export CO_2 and to store it abroad. This assumption allows for the use of carbon capture technologies and limits the quantity of carbon that can be captured. It is a significant assumption since it allows the model to use carbon-emitting technologies in the energy mix while still being able to reach carbon neutrality.

The model was simulated for only one year. While running it for multiple years (or for slight modifications of the data related to the same year) could produce more robust results, the focus was not primarily on achieving pinpoint accuracy regarding installed capacity. Instead, the goal was to assess the impact of specific hypotheses (namely the costs linked to H_2 imports, and the distance between the offshore cluster and the coastal one, see Section 4) and to gain a deeper understanding of the system's dynamics (Section 5).

7. Conclusion and future works

In this work, the primary goal was to determine the most effective method for transporting offshore energy to shore. Specifically, the study aimed to assess whether transporting part of the energy as hydrogen would be advantageous for the Belgian energy system. To achieve this, the Belgian energy system for 2050 was modelled and divided into three distinct geographical areas: offshore, coastal, and inland. Each area was assigned its own set of technologies. The model needs to satisfy the demand for three different energy carriers (electricity, hydrogen, and natural gas) while achieving carbon neutrality.

To assess the benefits of producing offshore hydrogen, two simulations were compared: one where only electricity is produced offshore and another where both electricity and hydrogen are produced offshore. Under the most conservative assumption about the potential of renewable energy (the base scenario), there is no benefit to allowing offshore hydrogen production. However, with more relaxed assumptions about renewable potential (the High Renewable scenario), the results show that producing hydrogen offshore incentivises the installation of more offshore wind turbines, increasing their capacity factors. Overall hydrogen production rises, leading to a total system cost reduction of 25 M€/year.

Furthermore, a sensitivity analysis was conducted on two factors: the impact of H_2 prices and the distance between the offshore area and the coast.

Regarding the price of H_2 imports, the production of offshore hydrogen increases up to a price of 105 €/MWh, leading to a rise in total production from electrolysers. This increase reaches 6.42 TWh of hydrogen produced under the conservative assumption on renewable potential and up to 18.9 TWh with more relaxed assumptions on renewable potential. This results in cost savings of 8.49 M€/year for the base scenario and 83.96 M€/year when hydrogen can be produced offshore. Above 105 €/MWh, steam methane reforming (SMR) with post-combustion carbon capture technologies becomes cost-competitive and the primary producer of hydrogen within the model.

Regarding the distance between the offshore area and the coast, as the distance increases, the model tends to decrease the capacity of installed wind turbines because the cost of interconnection becomes too expensive. However, this decrease is slowed when offshore hydrogen can be produced. In the base scenario, offshore wind turbine capacities remain at their maximum potential up to a distance of 750 km. Offshore hydrogen production at this distance exceeds 6 TWh (compared to almost non-existent production at 40 km), resulting in a cost difference of 65.58 M€/year at 750 km.

In the high renewable scenario, since the model has sufficient inland electricity to meet demand, offshore installations fall to zero at the longest distance studied.

Overall, the analyses tend to show that depending on several important factors (distance to the coast, price of hydrogen imports, solar and wind capacity), offshore H_2 production, and in general power-to-H_2, can contribute effectively to a decarbonised energy system and decrease slightly the total cost of the system. However, the import of H_2 remain necessary to meet the demand.

This work can be extended through several interesting paths. As the potential of renewable energy seems to be the most important factor for the production of offshore hydrogen, extending this model by adding more countries with more renewable resources could lead to interesting results. This would offer greater precision while handling the exchanges between countries for all commodities as well.

Furthermore, the granularity of the Belgian model itself can be more precise. This can be achieved by modelling both transmission and distribution networks for hydrogen, natural gas and electricity. This would allow Belgian authorities to have a precise insight of the future of the different networks. Other improvements to the model could include making energy demand endogenous for heating and transport, adding missing energy vectors such as biomass, oil, and coal, and studying pathways from the present to the solution for 2050.

Finally, a focus on the potential of the North Sea as an individual cluster can also be considered. As it is a key spot for renewable production (wind) and it can be used an exchange spot between countries.

CRediT authorship contribution statement

Jocelyn Mbenoun: Writing – original draft, Visualization, Validation, Methodology, Investigation, Formal analysis, Conceptualization. **Amina Benzerga:** Validation, Writing – original draft, Writing – review & editing, Visualization. **Bardhyl Miftari:** Conceptualization, Methodology, Validation, Writing – original draft, Writing – review & editing, Visualization. **Ghislain Detienne:** Writing – review & editing, Conceptualization. **Thierry Deschuyteneer:** Writing – review & editing, Conceptualization. **Juan Vazquez:** Writing – review & editing, Conceptualization. **Guillaume Derval:** Writing – review & editing, Supervision, Methodology, Formal analysis. **Damien Ernst:** Writing – review & editing, Supervision, Methodology, Conceptualization.

Codes

All codes used in this scientific publication are available at the following DOI: https://doi.org/10.5281/zenodo.14264974.

Declaration of Generative AI and AI-assisted technologies in the writing process

During the preparation of this work the authors used chat.gpt for minor word checks and rephrasing. After using this tool, the authors reviewed and edited the content as needed and take full responsibility for the content of the publication.

Declaration of competing interest

The authors declare the following financial interests/personal relationships which may be considered as potential competing interests: Jocelyn Mbenoun, Ghislain Detienne, Thierry Deschuyteneer, Juan Vazquez, Guillaume Derval reports financial support was provided by Service Public Fédéral Economie - Belgique. Ghislain Detienne, Thierry Deschuyteneer, Juan Vazquez reports a relationship with Fluxys that includes: employment. If there are other authors, they declare that they have no known competing financial interests or personal relationships that could have appeared to influence the work reported in this paper.

Acknowledgments

The authors gratefully acknowledge the support of the Federal Government of Belgium through its Energy Transition Fund and the INTEGRATION project.

Appendix

See Tables 2–12.

Data availability

Data will be uploaded on Zenodo upon acceptance. It is available on request in the meantime.

Table 2
Technical parameters used for conversion nodes. The reference commodity for each nodes is given in the second column.

n	Commodity r	$\underline{\kappa}^n$ GW or kt/h	$\bar{\kappa}^n$ GW or kt/h	κ^n_{tot} TWh/y or Mt/y	α^n –	μ^n –	Δ^n_+/Δ^n_- –	Source
PV	Electricity	0.0	50.0	–	0.0	0.0	–	[6]
WON		0.0	8.0	–	0.0	0.0	–	[6]
WOFF		0.0	9.0	–	0.0	0.0	–	[6]
NK		0.0	0.0	–	3.0/52.0	0.0	0.01/0.01	[12,35]
FC		0.0	∞	–	0.0	0.0	1.0/1.0	[12,34,35]
CCGT		0.0	∞	–	2.0/52.0	0.4	1.0/1.0	[12,35]
OCGT		0.0	∞	–	0.75/52.0	0.2	1.0/1.0	[12,35]
EP	H_2	0.0	∞	–	2.0/365.0	0.05	1.0/1.0	[12,36]
SMR		0.0	∞	–	0.0	0.0	1.0/1.0	[12,46]
MT	CH_4	0.0	∞	–	0.0	0.0	0.01/0.01	[12]
BMT		0.0	$1.5 \cdot \kappa^n_{tot}$	14.08	10/365	0.5	0.01/0.01	[33,35]
DAC	CO_2	0.0	∞	–	0.0	0.0	1.0/1.0	[47]
PCCC		0.0	∞	–	0.0	0.0	1.0/1.0	[12]
DU	H_2O	0.0	∞	–	0.0	1.0	0.0/0.0	[12]

Table 3
Conversion factors for each conversion technology. These efficiencies are used in Eqs. (1). The sources for each efficiency are listed in the last column. The units of the reference commodity for each technology are in the second column while the values for the used conversion factors are given in the remaining columns. Note that only 90% of CO_2 can be captured by the PCCC from the CO_2 emitted by gas turbines (CCGT or OCGT). For electrolyser plants, the electricity used for compressing hydrogen is accounted for within the term ϕ_{el}.

	Unit of r	ϕ_{el} GWh_{el}	ϕ_{H_2} GWh_{H_2}	ϕ_{CH_4} GWh_{CH_4}	ϕ_{CO_2} kt_{CO_2}	ϕ_{H_2O} kt_{H_2O}	ϕ_{fuel} GWh_{fuel} or kt_{fuel}	Source
NK	GWh_{el}	1.00	–	–	–	–	0.38	[12,35]
FC			0.58	–	–	2.13	–	[12,34,35]
CCGT			–	0.6	2.97	–	–	[12,35]
OCGT			–	0.45	2.23	–	–	[12,35]
EP	GWh_{H_2}	0.74	1.00	–	–	3.70	–	[12,36]
SMR		50.00		0.76	3.76	–	–	[12,46]
MT	GWh_{CH_4}	–	0.98	1.00	4.95	–	–	[12]
BMT		16.67	–		4.95	–	0.33	[33,36]
DAC	kt_{CO_2}	0.56	–	–	1.00	–	–	[47]
PCCC		2.42	–	–	0.90	–	–	[12]
DU	kt_{H_2O}	0.004	–	–	–	1.00	–	[12]

Table 4
Economic parameters used to model conversion nodes. CAPEX of offshore electrolysers considers the cost of the offshore platform on top of the cost of the technology.

n	$CAPEX^n$ M€/GW or M€/kt/h	θ_f^n M€/GW-yr or M€/(kt/h)-yr	θ_v^n €/MWh or €/t	χ_i^n €/MWh & €/t or €/t	L^n year	Source
PV	610.00	13.00	0.00	–	25	[34]
WON	943.00	12.00	0.18	–	25	[34]
WOFF	1995.00	32.00	0.39	–	25	[34]
NK	4700.00	105.00	7.8	1.69	50	[34]
FC	2668.00	40.00	1.04	–	20	[34]
OCGT	412.00	7.42	4.50	–	25	[35]
CCGT	750.00	15.00	1.73	–	30	[34]
EP onshore	333.33	6.67	0.00	–	35	[36]
EP offshore	502.13	6.67	0.00	–	35	[36,48,49]
SMR	805.00	37.80	0.17	–	25	[46]
MT	291.4	10.00	1.10	–	20	[34]
BMT	1733.00	165.18	0.00	10.23	15	[33,36]
DAC	4000.00	20.00	0.00	–	30	[47]
PCCC	3150.0	0.00	0.00	–	20	[12]
DU	28.08	0.0	0.32	–	20.0	[50]

Table 5
Capacity parameters used for storage nodes.

	$\underline{\epsilon}^n$ GWh	$\bar{\epsilon}^n$ GWh	$\underline{\kappa}^n$ GW	$\bar{\kappa}^n$ GW	Source
PHP	5.3	5.3	1.3	1.3	[6]
CH_4S	8000	8000	7	7	Fluxys

Table 6
Technical parameters used for storage nodes.

	η_S^n	η_+^n	η_-^n	ρ^n	ξ	ϕ_i^n $GWh_{elec}/GWh_{molecule}$	α^n	Source
Batteries	0.004	0.91	0.90	0.17	–	–	0.002	[37]
Pumped hydro	0.0	0.89	0.89	1.0	–	–	0.00	[35]
H_2O storage	0.0	1.0	1.0	1.0	–	0.00036	0.00	[12]
H_2 storage	1.0	0.98	0.98	1.0	0.1	0.0	0.0	[12,36]
CH_4 storage	1.0	0.99	0.99	0.5	–	–	0.0	[12]
CO_2 storage	1.0	1.0	1.0	1.0	0.2	–	0.0	[12]

Table 7
Technical parameters of flexibility nodes.

	$\underline{\epsilon}^n$ GWh	$\bar{\epsilon}^n$ GWh	$\underline{\kappa}^n$ GW	$\bar{\kappa}^n$ GW	γ^n h	ω^n h	Source
Load shifting	1.5	1.5	1.5	1.5	0	–	[6]
Linepack	39.44	39.44	9.86	9.86	6	–	Fluxys
Load shedding 1 h	–	–	0.128	0.2	0	1	[6]
Load shedding 2 h	–	–	0.446	0.7	0	2	[6]
Load shedding 4 h	–	–	0.534	0.607	0	4	[6]
Load shedding 8 h	–	–	0.383	0.6	0	8	[6]
Load shedding 24 h	–	–	0.191	0.3	0	24	[6]

Table 8
Economic parameters used to model flexibility nodes (2050 estimates).

	$CAPEX_{stock}$ M€/GWh or M€/kt	$CAPEX_{flow}$ M€/GWh or M€/kt	ϑ_f^n M€/GW or M€/kt/h	θ_f^n M€/GW or M€/kt/h	ϑ_v^n M€/GWh or M€/kt	θ_v^n M€/GWh or M€/kt	L^n years	Source
Batteries	75.00	60.00	0.00	0.54	0.00	1.6e−3	25	[37]
Pumped hydro	0.00	0.00	0.00	20.00	0.00	0.00	50	[34,37]
H_2O storage	0.065	1.56	0.001	0.031	0.00	0.00	30	[12]
H_2 storage	8.40	0.00	0.55	0.00	0.00	0.00	30	[37]
CH_4 storage	0.10	0.00	0.003	0.00	0.00	0.00	80	[12]
CO_2 storage	0.10	0.00	0.00	0.00	0.00	0.00	20	[12]
Load shedding 1 h	–	–	–	80	–	2.50	–	[6]
Load shedding 2 h	–	–	–	80	–	2.00	–	[6]
Load shedding 4 h	–	–	–	80	–	1.50	–	[6]
Load shedding 8 h	–	–	–	80	–	1.00	–	[6]
Load shedding 24 h	–	–	–	80	–	0.50	–	[6]

Table 9
Economic and technical parameters used to model import or export nodes.

n	$\underline{\kappa}^n$ GW or kt/h	v_t^n €/MWh or €/t	ϕ_{CO_2} GWh_{CH_4}/kt_{CO_2}	Source
NGNO	18.35	50.00 + 0.83	–	[38,41]
NGUK	24.50	50.00 + 0.84	–	[38,41]
NGFR	9.37	50.00 + 0.22	–	[38,41]
NGDE	15.06	50.00 + 0.54	–	[38,41]
SMI	26.81	164.80	4.95	[12]
H_2NL	25.65	75.00	–	[51]
CO_2E	3.50	2.00	–	[12]

Table 10
Technical and economical parameters used to model the electricity import from neighbouring countries.

	$\underline{\kappa}^{n,WOFF}$ GW	$\underline{\kappa}^{n,WON}$ GW	$\underline{\kappa}^{n,PV}$ GW	$\underline{\kappa}^{n,NK}$ GW	$\underline{\kappa}^{n,HV}$ GW	$Length_{HV}$ km	β^n [–]	v_t^n M€/GWh
Denmark	23.00	6.7	22.2	0.0	2	600	0.01	0.0448
United Kingdom	100.592	39.755	93.538	5.6	2.4	150	0.01	0.0447
Netherlands	60.137	9.676	94.856	0.0	5.4	50	0.01	0.0463
France	43.446	40.802	158.048	15.2	8.3	50	0.01	0.0475
Germany	52.199	68.376	268.215	0.0	1	50	0.01	0.046
Luxembourg	0.0	0.534	0.726	0.0	1	50	0.01	0.0399

Table 11
Technical parameters of transmission nodes.

	$\underline{\kappa}^n$ GW	$\bar{\kappa}^n$ GW	Length km	ϕ_l^n	ϕ_l^n $GW_{el}/GW_{molecule}$	Source
Submarine HVAC	2.3	100	–	0.93	–	[6,52]
Inland HVAC	3	100	–	0.93	–	[6]
Submarine HVDC	0	100	40	0.98	–	[6]
Submarine H_2 pipeline	0	100	40	0.9992	0.015	[1]
Inland H_2 pipeline	0	100	47	0.9992	0.015	[1]
Inland natural gas pipeline	60.5	100	47	0.9992	–	Fluxys

Table 12
Economic parameters of transmission nodes.

	Length km	CAPEX M€/GW	θ_f^n M€/GW	θ_v^n M€/GWh	Lifetime year	Source
Submarine HVAC	40	4.57 * length + 217.2	6.00	1.00e−6	70	[6,12]
Inland HVAC	47	133.33	2.00	1.00e−6	70	[6,12]
Submarine HVDC	40	1 * length + 762.6	0.015 * CAPEX	1.00e−6	40	[6]
Submarine H_2 pipeline	40	0.227 * length	0.03 * CAPEX	1.00e−6	40	[1]
Inland H_2 pipeline	47	0.227 * length	0.03 * CAPEX	1.00e−6	40	[1]
Inland natural gas pipeline	47	0.0925 * length	0.03 * CAPEX	1.00e−6	40	Fluxys

References

[1] TYNDP 2022 - scenario export. 2022.
[2] Capros P, De Vita A, Tasios N, Siskos P, Kannavou M, Petropoulos A, Evangelopoulou S, Zampara M, Papadopoulos D, Nakos C, et al. EU reference scenario 2016-energy, transport and GHG emissions trends to 2050. 2016.
[3] Limpens G, Jeanmart H, Maréchal F. Belgian energy transition: what are the options? Energies 2020;13(1):261.
[4] Devogelaer D, Gusbin D, Duerinck J, Nijs W, Marenne Y, Orsini M, Pairon M. Towards 100% renewable energy in Belgium by 2050. 2012.
[5] Clymans W, Vermeiren K, Meinke-Hubeny F. How much renewable energy can be generated within the Belgian borders? (dynamic energy atlas). 2021, URL https://www.energyville.be/en/press/how-much-renewable-electricity-can-be-generated-within-belgian-borders-dynamic-energy-atlas.
[6] Elia. Roadmap to net zero Elia Group's vision on building a climate-neutral European energy system by 2050. 2021.
[7] The potential to reduce CO2 emissions by expanding end-use applications of electricity, 1018871. 2009.
[8] Adequacy and flexibility study for Belgium 2022 - 2032. 2021.
[9] Elia Group. Half-year results: Elia group on track to deliver crucial grid investments that will propel a sustainable energy transition. 2024, URL https://investor.eliagroup.eu/-/media/project/elia/shared/documents/press-releases/2024/20240724_pressreleaseeliagroupq2_en.pdf. Press release.
[10] Wang A, Jens J, Mavins D, Moultak M, Schimmel M, van der Leun K, Peters D, Buseman M, et al. Analysing future demand, supply, and transport of hydrogen. 2021.
[11] Berger M, Radu D, Fonteneau R, Deschuyteneer T, Detienne G, Ernst D. The role of power-to-gas and carbon capture technologies in cross-sector decarbonisation strategies. Electr Power Syst Res 2020;180:106039.
[12] Berger M, Radu D, Detienne G, Deschuyteneer T, Richel A, Ernst D. Remote renewable hubs for carbon-neutral synthetic fuel production. Front Energy Res 2021;9:671279.
[13] Maroufmashat A, Fowler M, Khavas SS, Elkamel A, Roshandel R, Hajimiragha A. Mixed integer linear programing based approach for optimal planning and operation of a smart urban energy network to support the hydrogen economy. Int J Hydrog Energy 2016;41(19):7700–16.
[14] Diéguez MS, Fattahi A, Sijm J, España GM, Faaij A. Linear programing formulation of a high temporal and technological resolution integrated energy system model for the energy transition. MethodsX 2022;9:101732.
[15] Miftari B, Berger M, Djelassi H, Ernst D. GBOML: Graph-based optimization modeling language. J Open Source Softw 2022;7(72):4158.
[16] Fourer R, Gay DM, Kernighan BW. A modeling language for mathematical programming. Manage Sci 1990;36(5):519–54.
[17] Hart WE, Watson J-P, Woodruff DL. Pyomo: modeling and solving mathematical programs in python. Math Program Comput 2011;3:219–60.
[18] Brown T, Hörsch J, Schlachtberger D. PyPSA: Python for power system analysis. 2017, arXiv preprint arXiv:1707.09913.
[19] Pfenninger S, Pickering B. Calliope: a multi-scale energy systems modelling framework. J Open Source Softw 2018;3(29):825.
[20] Mancarella P. MES (multi-energy systems): An overview of concepts and evaluation models. Energy 2014;65:1–17.
[21] Geidl M, Andersson G. Operational and structural optimization of multi-carrier energy systems. Eur Trans Electr Power 2006;16(5):463–77.
[22] Collins S, Deane JP, Poncelet K, Panos E, Pietzcker RC, Delarue E, Gallachóir BPÓ. Integrating short term variations of the power system into integrated energy system models: A methodological review. Renew Sustain Energy Rev 2017;76:839–56.

[23] Belderbos A, Valkaert T, Bruninx K, Delarue E, D'haeseleer W. Facilitating renewables and power-to-gas via integrated electrical power-gas system scheduling. Appl Energy 2020;275:115082.
[24] Otsuki T, Komiyama R, Fujii Y, Nakamura H. Temporally detailed modeling and analysis of global net zero energy systems focusing on variable renewable energy. Energy Clim Change 2023;4:100108.
[25] Bogdanov D, Farfan J, Sadovskaia K, Aghahosseini A, Child M, Gulagi A, Oyewo AS, de Souza Noel Simas Barbosa L, Breyer C. Radical transformation pathway towards sustainable electricity via evolutionary steps. Nat Commun 2019;10(1):1–16.
[26] Mathiesen BV, Lund H, Karlsson K. 100% renewable energy systems, climate mitigation and economic growth. Appl Energy 2011;88(2):488–501.
[27] Dadkhah A, Van Eetvelde G, Vandevelde L. Optimal investment and flexible operation of power-to-hydrogen systems increasing wind power utilisation. In: 2022 IEEE international conference on environment and electrical engineering and 2022 IEEE industrial and commercial power systems Europe. EEEIC/I&CPS Europe, IEEE; 2022, p. 1–6.
[28] Misyris G, Van Cutsem T, Møller J, Dijokas M, Estragués OR, Bastin B, Chatzivasileiadis S, Nielsen A, Weckesser T, Østergaard J, et al. North sea wind power hub: System configurations, grid implementation and techno-economic assessment. 2020, arXiv preprint arXiv:2006.05829.
[29] Ibrahim OS, Singlitico A, Proskovics R, McDonagh S, Desmond C, Murphy JD. Dedicated large-scale floating offshore wind to hydrogen: Assessing design variables in proposed typologies. Renew Sustain Energy Rev 2022;160:112310.
[30] Singlitico A, Østergaard J, Chatzivasileiadis S. Onshore, offshore or in-turbine electrolysis? Techno-economic overview of alternative integration designs for green hydrogen production into offshore wind power hubs. Renew Sustain Energy Transit 2021;1:100005.
[31] Thommessen C, Otto M, Nigbur F, Roes J, Heinzel A. Techno-economic system analysis of an offshore energy hub with an outlook on electrofuel applications. Smart Energy 2021;3:100027.
[32] Miftari B, Berger M, Derval G, Louveaux Q, Ernst D. GBOML: a structure-exploiting optimization modelling language in python. Optim Methods Softw 2023;1–30. http://dx.doi.org/10.1080/10556788.2023.2246169, arXiv:https://doi.org/10.1080/10556788.2023.2246169.
[33] Quelle place pour le biométhane injectable en Belgique? 2019.
[34] ASSET study on technology pathways in decarbonisation scenarios. 2018.
[35] Technology data - generation of electricity and district heating. 2016.
[36] Technology data - renewable fuels. 2017.
[37] Technology data - energy storage. 2018.
[38] Europe GI. Aggregated gas storage inventory. 2021, URL https://agsi.gie.eu/.
[39] Assessing the benefits of a pan-European hydrogen transmission network. 2023.
[40] Analysing future demand, supply, and transport of hydrogen. 2021.
[41] Fluxys. Fluxys Belgium - tarifs de transport. 2021, URL https://www.fluxys.com/fr/natural-gas-and-biomethane/empowering-you/tariffs/tariff_fluxys-belgium-tra-2021.
[42] Koivisto M, Gea-Bermúdez J, Sørensen P. North sea offshore grid development: combined optimisation of grid and generation investments towards 2050. IET Renew Power Gener 2020.
[43] Electricity ten year statement 2015 - appendix E (technology). 2015.
[44] Elia. Load and load forecasts - total load. 2023, URL https://www.elia.be/en/grid-data/load-and-load-forecasts.
[45] information administration EUE. Natural gas explained. Factors affecting natural gas prices. 2023, URL https://www.eia.gov/energyexplained/natural-gas/factors-affecting-natural-gas-prices.php.
[46] Consortium H. The hydrogen for Europe study. 2022, URL https://www.hydrogen4eu.com/_files/ugd/2c85cf_e934420068d44268aac2ef0d65a01a66.pdf.
[47] Technology data - carbon capture, transport and storage. 2021.
[48] IEA. Offshore wind outlook 2019. Technical report, 2019.
[49] Gea-Bermúdez J, Bramstoft R, Koivisto M, Kitzing L, Ramos A. Going offshore or not: Where to generate hydrogen in future integrated energy systems? Energy Policy 2023;174:113382.
[50] Solution AW. Desalination technologies and economics: CAPEX, OPEX & technological game changers to come. 2016, URL https://web.archive.org/web/20201123110805/https://www.cmimarseille.org/sites/default/files/newsite/library/files/en/1.6.%20C.%20Cosin_%20Desalination%20technologies%20and%20economics_%20capex,%20opex%20and%20technological%20game%20changers%20to%20come%20-ilovepdf-compressed.pdf.
[51] Backbone EH. Estimated investment & cost. 2024, URL https://ehb.eu/page/estimated-investment-cost.
[52] Berger M, Radu D-C, Ryszka K, Ernst D, Fonteneau R, Detienne G, Deschuyteneer T. The role of hydrogen in the dutch electricity system. 2020.